October 2007

Office of Long Island Sound Programs
FINAL REPORT, GRANT LI-97100901

Application of Remote Sensing Technologies for the Delineation and Assessment of Coastal Marshes and their Constituent Species

Principal Investigators

Dr. Daniel Civco
University of Connecticut
Department of Natural Resource Management and Engineering
1376 Storrs Road, U-87
Storrs, CT 06269-4087
Phone: (860) 486-2840
Fax: (860) 486-5408
Email: daniel.civco@uconn.edu

Dr. Martha Gilmore
Wesleyan University
Department of Earth and Environmental Sciences
265 Church Street
Middletown, CT 06459-0139
Phone: (860) 685-3129
Fax: (860) 685-3651
Email: mgilmore@wesleyan.edu

Co-Investigators

Sandy Prisloe UConn, Haddam
Emily Wilson, UConn, Haddam
James Hurd, UConn, Storrs

Project Summary

Coastal wetlands are a critical component of the Long Island Sound ecosystem. However, over the past century, a significant amount of these wetlands has been lost due to development, filling, and dredging, or damaged due to anthropogenic disturbance and modification. Global sea level rise is also likely to have a significant impact on the condition and health of coastal wetlands, particularly if the wetlands have no place to migrate due to dense coastal development (Donnelly and Bertness, 2001). In addition to physical loss of marshes, the species composition of marsh communities is changing. *Spartina alterniflora* (salt cordgrass) and *Spartina patens* (salt marsh hay), once the dominant species of New England salt marshes, are being replaced by monocultures of *Phragmites australis* (Barrett and Prisloe, 1998; Orson, 1999). During the past 30-50 years, *P. australis* is estimated to be spreading at a rate of 1-3 percent per year (Niering *and Warren*, 1980; Warren, 1994). It has been estimated that approximately 10 percent of Connecticut's tidal wetlands are dominated by *P. australis* and further evidence identifies approximately 50 percent of tidal and brackish wetlands in Connecticut as sites of *P. australis* invasion (Niering and Warren, 1980; Roman *et al.*, 1984; Chambers *et al.*, 1999). *P. australis* outcompetes other marsh species in areas with increased fresh water, nitrogen and sediments and is positively correlated with marsh fragmentation [*e.g.,* Moore *et al*., 1999; Bertness *et al*., 2002]. In response to the increase of *P. australis* in many marshes, The Nature Conservancy, the CT DEP and other organizations have instituted efforts (commencing in the 1980s) to restore marsh health, including the control of *P. australis* in some areas. The response of marshes to control activities has included both an increase of non-*Phragmites* marsh species and *P. australis* reinvasion (Farnsworth and Meyerson, 1999). With the mounting pressures on coastal wetland areas, it is becoming increasingly important to identify and inventory the current extent and condition of coastal marshes located on the Long Island Sound estuary, identify techniques to

track changes in the condition of wetlands over time, and monitor the effects of habitat restoration and management.

The goal of this project was to examine the spatial, spectral, and temporal aspects of coastal marsh vegetation characterization, identification, and delineation along Long Island Sound using both remote sensing and *in situ* radiometry data. Issues addressed include determining the effectiveness of various types of remote sensing data to identify the extent of coastal wetlands, identifying dominant coastal wetland vegetation, including the invasive *Phragmites australis* at select marsh locations, assessing the potential impact of adjacent upland anthropogenic activity on coastal marsh health and sustainability, and providing recommendations for future coastal wetland mapping efforts. Major tasks include the delineation and monitoring of coastal marshes from moderate resolution (30 m/pixel) Landsat remote sensing imagery, identification of vegetative species within five select marshes from high spatial resolution (<3 m/pixel) QuickBird satellite imagery, ADS40 and John Deere AgriServices aircraft-based remote sensing imagery, development of a spectral library of dominant tidal marsh plant species throughout the growing season, determination of optimal spatial, spectral, and temporal resolutions for coastal wetland system characterization, and provide information online regarding the results of the work described here.

Project Period: April 1, 2004 – December 31, 2006

Project Description

The goal of this project was to use remote sensing to identify and delineate the extent of coastal marshes along the Connecticut and New York shores of Long Island Sound and distinguish among various types of dominant marsh vegetation within select marshes. This was accomplished through the use of Landsat Thematic Mapper and Enhanced Thematic Mapper moderate spatial resolution, public domain satellite imagery for the Sound-wide portion of the project with the more detailed assessment of the spatial extent of dominant marsh plant species using QuickBird, ADS40, and John Deere AgriServices high spatial resolution commercial remote sensing imagery combined with *in situ* field studies. The project consisted of the following four distinct tasks: 1) general delineation and assessment of coastal marshes, 2) identification of dominant vegetative species within select marshes, 3) recommendations for the optimal spatial, spectral, and temporal resolutions for coastal wetland system characterization and 4) web-based information dissemination of project results. A description of each task is provided in the following sections:

The goals of the work reported here, therefore, were to:

- identify and delineate coastal marshes (CT and north shore of Long Island, NY) using moderate resolution satellite imagery;
- assess the marshes in the context of surrounding land cover, impervious surfaces and potential for future migration as a response to sea level rise;
- create a library of *in situ* spectral measurements for dominant marsh plant species throughout the growing season;

- distinguish among various types of dominant marsh vegetation using high spatial resolution commercial remote sensing imagery combined with *in situ* field studies at five select tidal marsh sites;
- determine the optimal spatial, spectral, and temporal resolutions of imagery for coastal wetland system characterization;
- provide the results of the research through web access and educational programs.

Activities & Accomplishments

Task 1. Delineation and monitoring of coastal marshes

One of the major goals of this study was to develop a technique that uses moderate resolution imagery to map the location and extent of coastal marshes within the Long Island Sound estuary. Two sources of satellite imagery were examined to assess their efficacy to map adequately the tidal marshes of Long Island Sound. These include Landsat (both the Enhanced Thematic Mapper (ETM)/Thematic Mapper (TM) sensors) and ASTER[1] imagery.

<u>September 8, 2002 Landsat ETM Classification</u>

A September 8, 2002 Landsat ETM image was used as the primary image source for the classification of coastal wetlands throughout the Long Island Sound region. Preprocessing of this image consisted of mosaicking the WRS Path 13, Row 31 and Row 32 and Path 12 Row 31 scenes to create a seamless image that covers the entire Long Island Sound region. The WRS Path 12 Row 31 scene was acquired July 31, 2002 and substantially overlaps the September 8, 2002 scenes which provides a comparison of the repeatability of the classification technique used and discussed in a later section of this report. This image was further processed to decrease the total amount of data to be classified by focusing the analysis on only the coastal areas based on proximity to water (including Long Island Sound, rivers, and larger tidal creeks). Figure 1 provides an example of a portion of the Landsat ETM mosaic used for the classification following the extraction of the analysis area. An integrated classification approach which uses both pixel-based and object-based classification techniques was utilized to identify coastal wetlands in the analysis area.

Pixel-based classification. The pixel-based technique consisted of using an ISODATA "Cluster-busting" approach. In this technique, ISODATA clustering is used to identify potential categories of interest. Based on the number of clusters selected by the user to be identified, the computer places pixels into groups based on their spectral characteristics. The user then identifies and labels the clusters into a land cover category. Those clusters not readily identified are placed into an "other" category, extracted from the Landsat image and reclassified. This process was repeated four times. The results of the four cluster-busting procedures were recoded and combined to generate a final classification layer where each pixel is labeled as water, tidal marsh, and upland. To remove many of the isolated coastal marsh pixels falsely identified in the upland regions, and to smooth the overall result, a 3x3 pixel neighborhood majority filter was used. This resulting layer serves as the pixel-based classification that is applied to the integration with the object-based classification described in the next section. A sample of the classification is provided in Figure 2.

[1] Advanced Spaceborne Thermal Emission and Reflection Radiometer

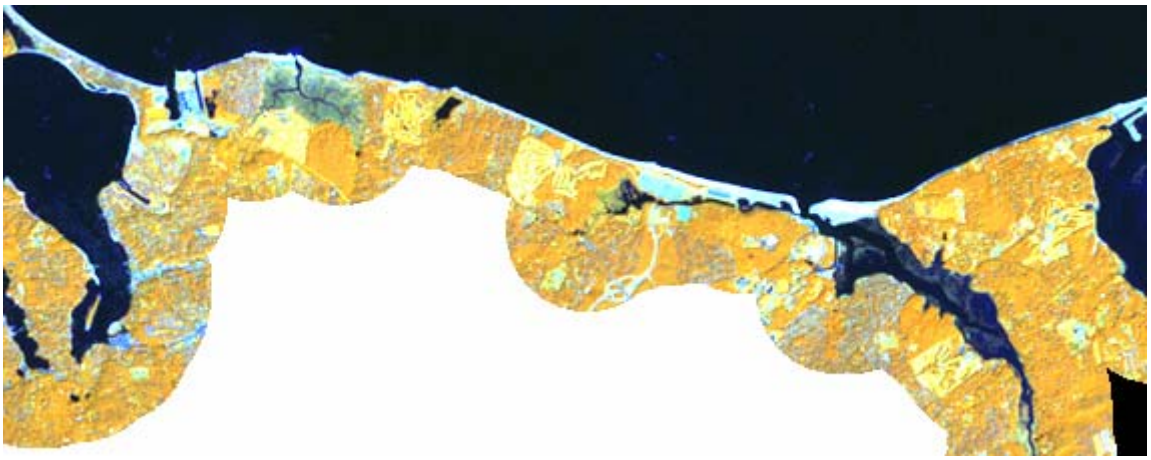

Figure 1. An example of the September 8, 2002 Landsat ETM image showing the analysis area extracted for a portion of the north shore of Long Island.

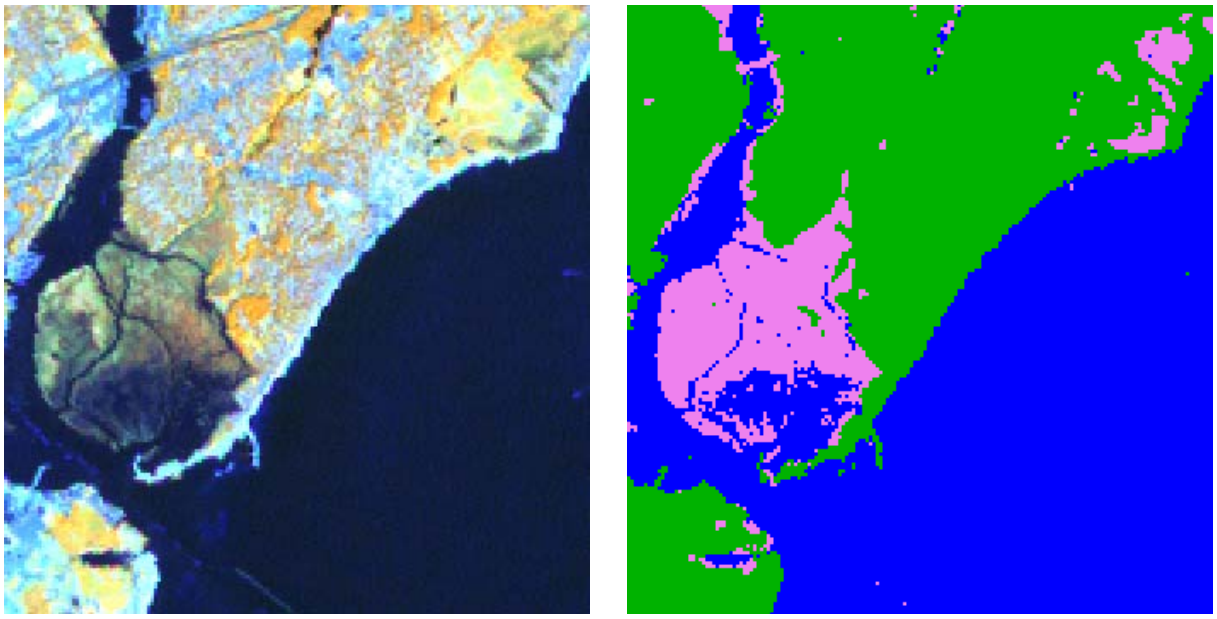

(a) September 8, 2002 Landsat image

(b) ISODATA per-pixel classification (coastal marshes are colored magenta)

Figure 2. ISODATA classification results on Landsat 30-meter resolution imagery for Wheeler Marsh located in Milford, Connecticut.

Object-based classification. In addition to the ISODATA "cluster busting" approach, an object-based classification was conducted using eCognition image processing software. Object-based classification is the process of classifying image objects rather then individual pixels. Image objects are created through multi-resolution segmentation which is the process of grouping contiguous pixels with similar qualities (*i.e.*, spectral, textural, spatial) based on information from one or more input layers. The benefit of object-based classification over per-pixel classifiers is that the image objects contain more information than just spectral information

provided by single pixels. In addition, each image object also contains information regarding the texture, size, shape, and context of that image object to surrounding image objects. The spectral and spatial attributes of each image object are utilized to assign the object to a specific classification category, paralleling somewhat the human visual cognitive process.

Input data for the object-based classification consisted of the six September 8, 2002 Landsat ETM reflective bands, Landsat ETM thermal band, Landsat ETM panchromatic band, derived NDVI (Normalized Difference Vegetation Index), a measure of plant biomass, principal components 1, 2, 4, and 6 (which is a technique used to reduce multidimensional data sets to lower dimensions and highlight certain land cover features for analysis), and a derived wetness layer (Landsat ETM band 5 – band 2). To generate the image objects using multi-resolution segmentation, only four Landsat ETM reflective bands (red, NIR, SWIR1 and SWIR2), NDVI (a greenness layer), principal component 1 (a brightness layer), and the wetness layer were used. These layers were equally weighted in their contribution to the segmentation process.

A general image segmentation was performed first to produce larger image objects which were used in a basic binary classification to separate upland objects from water objects. The results of this classification were used to assist with a more detailed classification process based on smaller image objects. eCognition allows for the creation of objects at various segmentation resolutions (sizes) depending on user specified variables. These include a scale parameter which determines the maximum size of the objects and the composition of the homogeneity criterion which uses settings of color, shape, smoothness and compactness that roughly determine the shape of the objects using spectral and shape information. The assignment of these parameters to generate image objects is based on knowledge of the software, input data used, the classification procedure to be followed, and what features are to be identified. For the generation of higher image objects (considered level 2 image objects by eCognition since larger objects have a larger level value) from the seven input layers used in the segmentation process, the scale parameter was set to 75, color 0.9 (from 0 to 1), shape 0.1 (color and shape must sum to 1), smoothness 0.5 and compactness 0.5 (smoothness and compactness must sum to 1). Since the color parameter was set much higher then the shape parameter, the spectral information from the input layers was the most significant contributor to the creation of these level 2 image objects.

To classify the level 2 image objects into upland or water, the wetness layer was used exclusively as the identifying feature. Data exploration of the image objects identified a wetness value of 20.13 as a probable threshold between water and upland objects. Tidal wetlands are expected to fall in one or the other category based on their level of wetness. To assign objects to a specific class, a fuzzy rule was used where the center point of the membership function was assigned a value of 20.13 with a range of 19.13 to 21.13. To identify water objects, any segment with a value larger then 21.13 was absolutely classified as water with a decreasing function slope to 19.13 (Figure 3a). Inversely, uplands were identified as any image object having a wetness value below 19.13 with a decreasing function slope to 21.13 (Figure 3b). By using a fuzzy rule, those image objects bordering between water and upland (*i.e.*, wetness value between 19.13 and 21.13) are more easily recognized. Figure 4 shows an example of the result of this level of object-oriented classification.

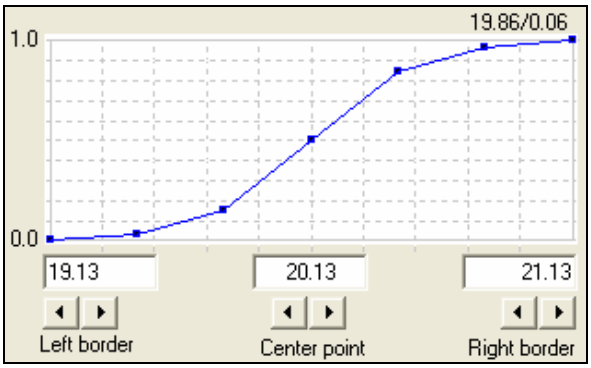

(a) Membership function used to identify water objects

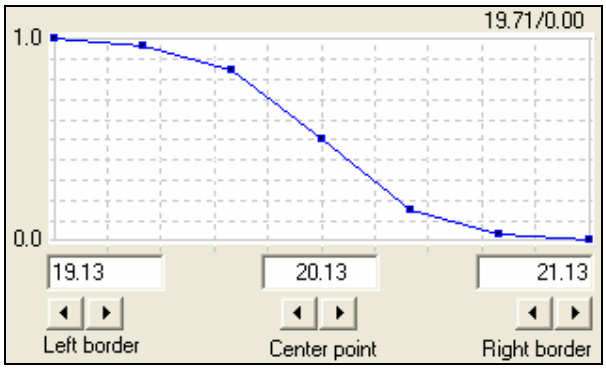

(b) Membership function used to identify upland objects.

Figure 3. Fuzzy rule membership functions used to classify level 2 image objects into water or upland categories.

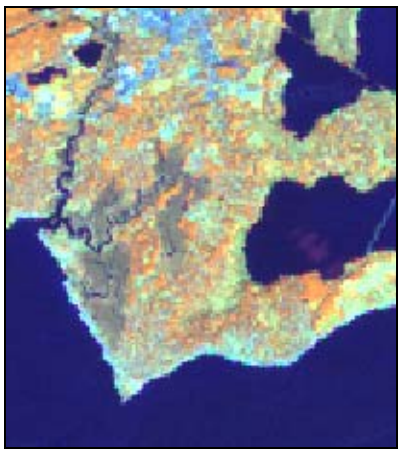

Landsat ETM image bands 4, 5, 3 displayed

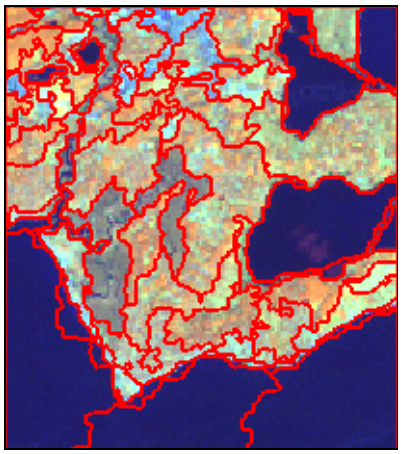

Landsat ETM image with Level 2 image objects outlined in red

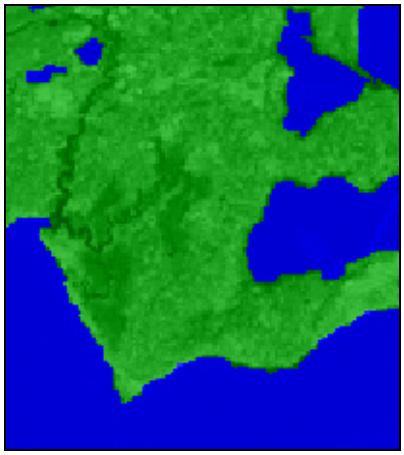

Level 2 object-oriented classification (green is upland, blue is water)

Figure 4. Sample of the Level 2 object-oriented classification. Green represents upland image objects, blue are water image objects.

To extract additional thematic information, a more detailed image object layer was created (level 1). As with the generation of the larger image objects in the level 2 segmentation, the same seven input layers were used in the level 1 segmentation process. The scale parameter, however, was set to 15 to generate smaller objects, color 0.9, shape 0.1, smoothness 0.5 and compactness 0.5. During the creation of multiple levels of image objects (*i.e.*, level 1 and level 2), the more detailed objects (level 1) will be nested within larger objects (level 2). Any characteristic of a larger image object can be applied to the smaller image objects nested within it and, therefore, aid in the classification of the more detailed image objects.

Since the classification of image objects can utilize spatial information such as the texture, size, shape, and context in addition to spectral information, it can become increasingly difficult to identify which characteristic of an object are most important or significant for identifying the features of interest. To assist in the determination of these characteristics, See5, a data mining

tool developed by RuleQuest Research[2], was used. See5 analyzes and extracts patterns to identify those input characteristics that are deemed most important for identifying features of interest. The output from See5 is a decision tree that can be re-created in eCognition and used to classify the image objects.

To develop the database, image object information from eCognition was exported to an ESRI polygon shapefile and representative objects were identified for each of the following land cover features: Water Rounded (ocean & lake), Water Elongated (tidal creeks), Low Marsh, High Marsh, High Marsh bright, Grass yellow, Grass green, Forest, Barren, Bright Development, Dark Development, Dense Development, and Sparse Development. Objects included information such as the mean value for each input data layer (*i.e.*, blue band, NIR band, NDVI, PCA 1, etc.), the standard deviation for each input data layer, object brightness, object area, object length, object width, object length to width ratio, object shape index, and object density. In all there were 35 unique characteristics that described each image object, and 2,294 objects were selected as training data. The attributes of these objects were saved in a database file and converted to a format usable by See5.

One of the options in See5 allows for *winnowing* the data. This process assesses the input characteristics and determines which contribute the most to the final classification decision tree. Essentially, the process *weeds out* those characteristics that are found not to be significant contributors to the classification and excludes them from the decision tree creation process. Of the 35 image object characteristics provided to See5, only 22 were used in the construction of the decision tree. Of these, only six were considered to by highly significant: mean band 5 (SWIR), mean NDVI, mean band 1 (blue), mean wetness, mean panchromatic, and mean band 2 (green). The output decision tree from See5 was then re-created in eCognition using membership functions similar to that used in the level 2 classification. See5 provided more branches of the decision tree is depicted in the eCognition classification decision tree shown in Figure 5. Since tidal marshes were the target feature, only those branches and thresholds that classified tidal marshes were used. If the branch continued to separate further other upland or water classes, a generic class was given and the branch ended. A sample of the result of the level 1 classification is provided in Figure 6.

Final classification. To produce a final coastal wetland classification, the results from the ISODATA "cluster-busting" and the object-oriented classification were combined. ERDAS Imagine's Knowledge Engineer was utilized for this purpose. The Knowledge Engineer is a GUI used to design a rule-based approach to classification that utilizes a decision tree. The decision tree is comprised of variables and a hierarchy of rules, which are conditional statements, to produce a final classification output. The decision tree used for this project is basic. Input variables consist of the final ISODATA classification and the object-oriented classification. In addition, the following data layers were also included to improve the final classification result: PCA1 (brightness), NDVI, Wetness, and elevation DEM. Output classes consisted of water, upland, low marsh, and high marsh. Figure 7 shows the design of the decision tree in the Knowledge Engineer.

[2] http://www.rulequest.com/see5-info.html

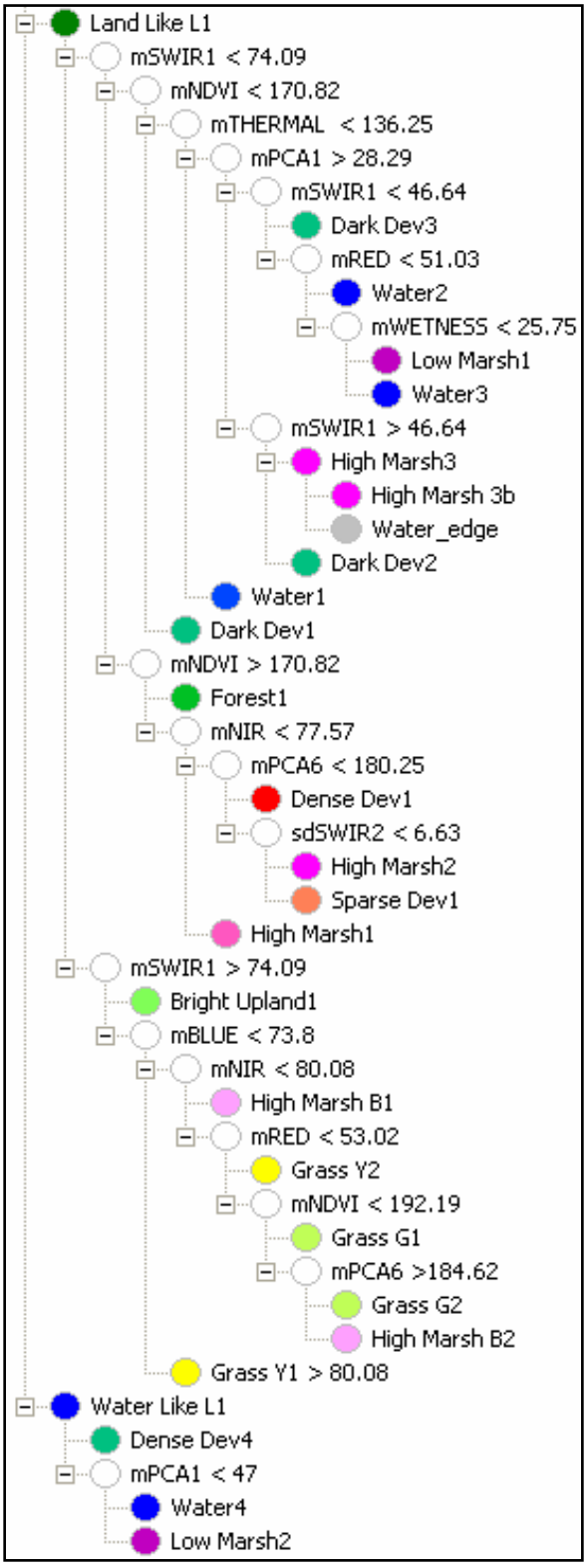

Figure 5. Classification decision tree created in eCognition based on thresholds generated from See5.

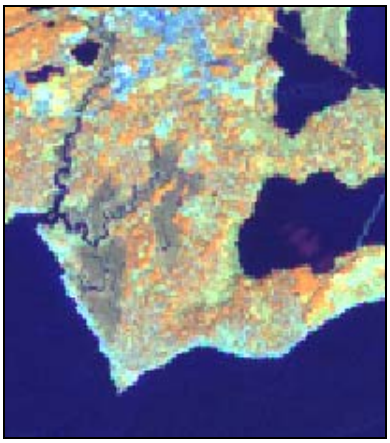

Landsat ETM image bands 4, 5, 3 displayed

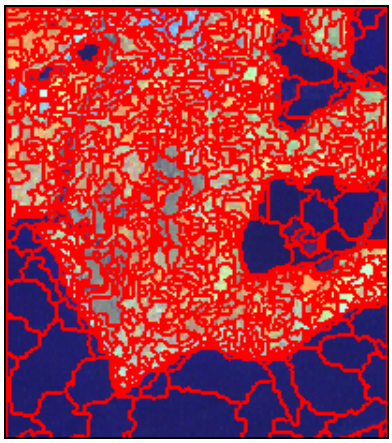

Landsat ETM image with Level 1 image objects outlined in red

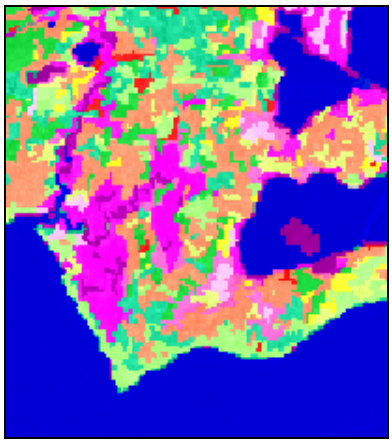

Level 1 object-oriented classification

Figure 6. Sample of the Level 1 object-oriented classification. Greens, yellows and orange represent upland image objects, blue are water image object, and magenta, purple and pink are tidal wetland objects.

To summarize the output results shown in Figure 7:

1. Water is classified using the Wetness layer and PCA1. Following an attempt to utilize the classified water from both the ISODATA classification and Object-based classification, it was determined that a pixel with a wetness value greater then or equal to 20.4 and PCA1 value less then or equal to 34 gave a superior result. Values were selected based on visual examination of the data layers.
2. Low Marsh is classified using the results of the ISODATA classification and the Object-based classification. In addition, elevation information was utilized. If the ISODATA classification equals marsh (ISODATA class 2) and the object-based classification equals low marsh (Object-based class 2) and the elevation is less than or equal to 5.33, then the pixel is assigned as low marsh. The elevation value was determined by selecting multiple points both within the marshes and uplands from the Landsat imagery then analyzed with the elevation data to identify an appropriate elevation threshold.
3. High Marsh is classified using a similar rule to the Low Marsh classification. In this case, however, the object-based class equals high marsh (Object-based class 3).
4. Upland is classified using three separate rules. The first rule (D1 in Figure 7) identifies a pixel as upland if the ISODATA classification equals upland (ISODATA class 3) and The Object-based classification equals upland (Object-based class 4) and the elevation is less than or equal to 5.33. These upland pixels occur at low elevations in close proximity to the coastal marshes and coastal waters. The second rule (D2 in Figure 7) assigns any pixel above an elevation of 5.33 as upland. This comprises the vast majority of the upland. pixels. The last rule (D3 in Figure 7) uses the NDVI layer to identify pixels of high vegetation biomass that are not wet. In this rule, the elevation is less than or equal to 5.33 and NDVI is greater then or equal to 191 when stretched to an 8-bit dataset. This rule was developed to capture more of the low lying upland pixels not captured using rule D1.

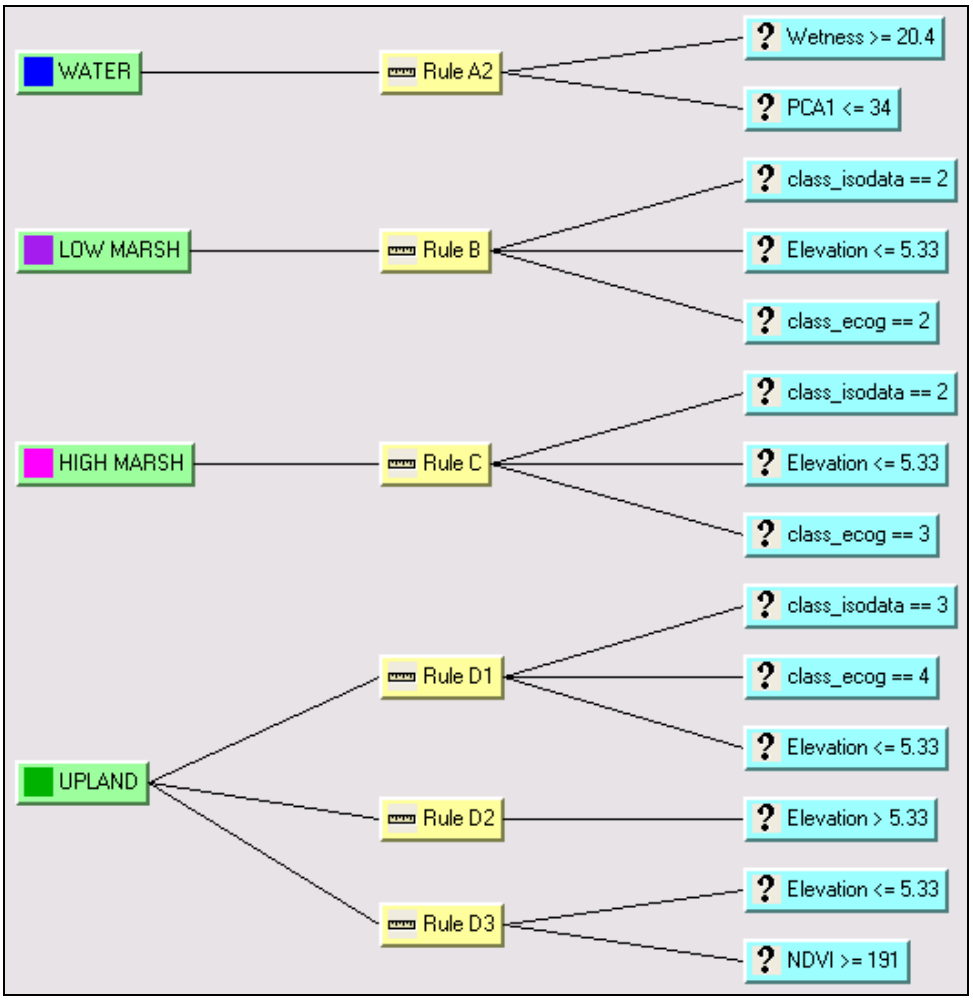

Figure 7. Graphic showing the design of the decision tree used to integrate the ISODATA classification with the object-based classification.

The order of rules in the knowledge base affects the classification results; in the Knowledge Engineer, lower rules in the hierarchy are superseded by rules located higher in the hierarchy. Pixels that meet the criteria of more than one rule are assigned the value identified by the top-most rule in the decision tree. The order of each rule in the decision tree is therefore important. It is also possible to have pixels not classified by any of the rules. Those pixels not placed in a land cover category based on the decision tree were extracted and classified using ISODATA to assign them to one of the final four categories. These pixels were merged with the integrated classification to produce a final tidal marsh classification map (Figures 8 and 9).

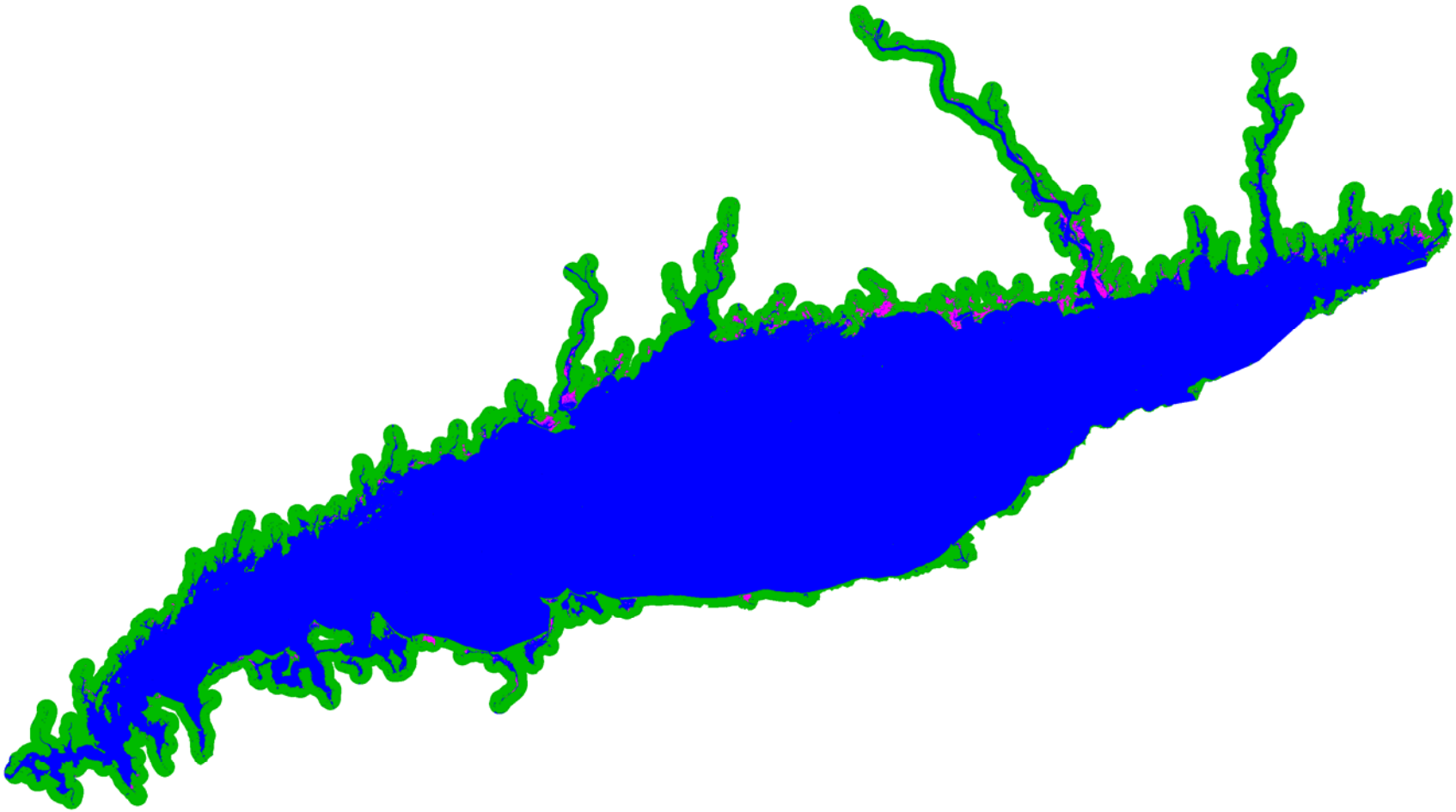

Figure 8. Final 2002 coastal wetland classification for Long Island Sound (water is blue (832,003 acres), upland is green (318,981 acres), high coastal marsh is magenta (9,563 acres), low coastal marsh is purple (2,563 acres)).

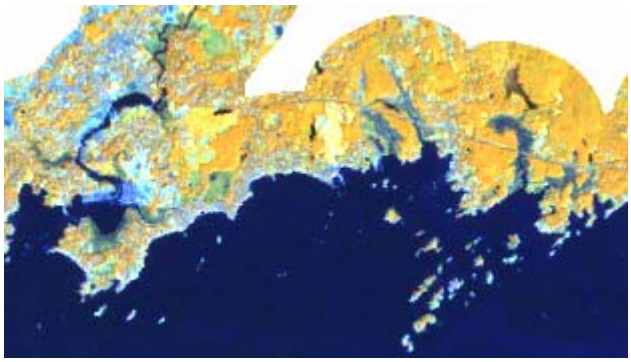

(a) September 8, 2002 Landsat ETM image, Branford and Guilford, Connecticut

(b) Coastal wetland classification, Branford and Guilford, Connecticut

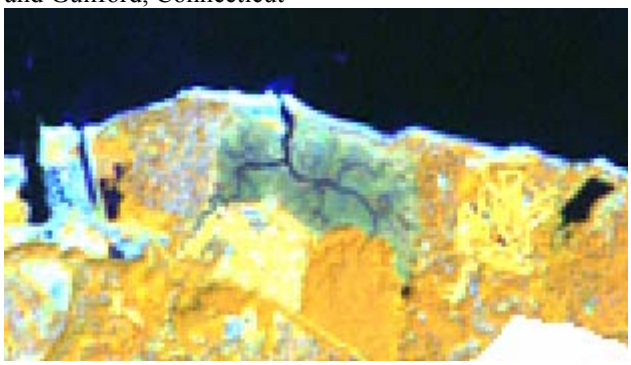

(c) September 8, 2002 Landsat ETM image, Crab Meadow, Huntington, New York (zoomed 2x)

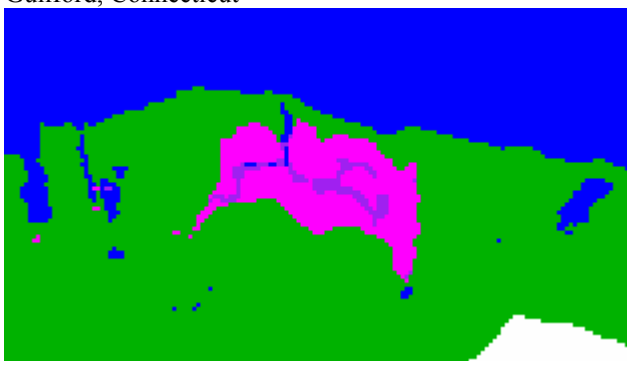

(d) Coastal wetland classification, Crab Meadow, Huntington, New York (zoomed 2x)

Figure 9. Close up examples showing the results of the final Landsat based coastal wetland classification**.**

Accuracy assessment consisted of the generation and *ground truth* labeling of 1,000 stratified random sample of points. These points were compared against the Landsat imagery and high resolution ADS40 imagery (for the Connecticut coast) in addition to utilizing Google Earth to help identify the land cover at each sample point. The points were labeled as one of the four land cover categories of water, low marsh, high marsh, and upland and used to produce the reference information. The reference information was compared with the classified information for each sample point to produce an error matrix to calculate user's (a measure of the reliability of an output map generated from a classification scheme) and producer's (a measure of the accuracy of a particular classification scheme) and overall classification accuracy and the Kappa coefficient[3] (Congalton and Green, 1999)**.** The results are reported in Table 1. As can be seen, the overall accuracy is high (92.90%) with the best classification accuracies being with the water category followed closely by the upland category. This is to be expected since most of the image is comprised of water which is a spectrally unique feature and is typically easily classified. The low marsh and high marsh categories show lower classification accuracies with most of the error occurring between these two classes.

[3] Cohen's Kappa Coefficient accounts for agreement due to chance alone. A value of kappa approaching 1.0 indicates very high agreement, a value approaching -1.0 indicates total disagreement, and a value near zero indicates agreement no better than that achieved by chance alone.

Table 1. Accuracy assessment of the September 8, 2002 Landsat classification.

	Reference					
Classified	**Water**	**Low Marsh**	**High Marsh**	**Upland**	**Totals**	**Users Accuracy**
Water	557	0	1	2	560	99.46%
Low Marsh	9	58	31	2	100	58.00%
High Marsh	0	8	80	15	103	77.67%
Upland	1	0	2	234	237	98.73%
Totals	567	66	114	253	1000	
Producers Accuracy	98.24%	87.88%	70.18%	92.49%		

Number Correct = 929 out of 1,000
Overall Accuracy = 92.90%
Overall Kappa Statistic = 0.8825

To reduce the influence of the water class on the accuracy assessment, a second assessment was conducted on a reduced dataset. The original classification was buffered 90 meters around the classified high and low marsh areas. This produced a classified image with a 90 meter-wide band around the coastal marsh areas producing an image with less water and upland influence to provide a better assessment of the accuracy of the coastal marsh areas (Figure 10). Similar to the previous assessment, a stratified random sample of points was selected, however, only 300 points were used. Table 2 provides the results. As can be seen, the overall accuracy has dropped (84.67%) due to the reduced amount of water in the assessed classification. Also of note is the slight increase in accuracy of the low and high marsh categories.

July 31, 2002 Landsat classification of eastern Long Island Sound

To classify the extreme eastern portion of the Sound, a separate Landsat scene (July 31, 2002) had to be acquired. Not only did this image serve to provide data for the classification of the eastern Sound, but also, due to the considerable overlap with the September 8, 2002 scene (Figure 11), it allowed for a comparison of the repeatability of the classification technique. The classification procedures followed for this July 31, 2002 scene were identical to the September 8, 2002 although different training areas were used for the object-based classification portion of the classification. There are more than 2 million pixels in the overlap area. Table 3 provides statistics of the classification agreement and disagreement of each of these pixels. As can be seen, 98.40% of the pixels agreed. The categories of highest agreement were with the water and upland categories. Again, these are the most abundant categories resulting in better agreement. The low marsh category showed

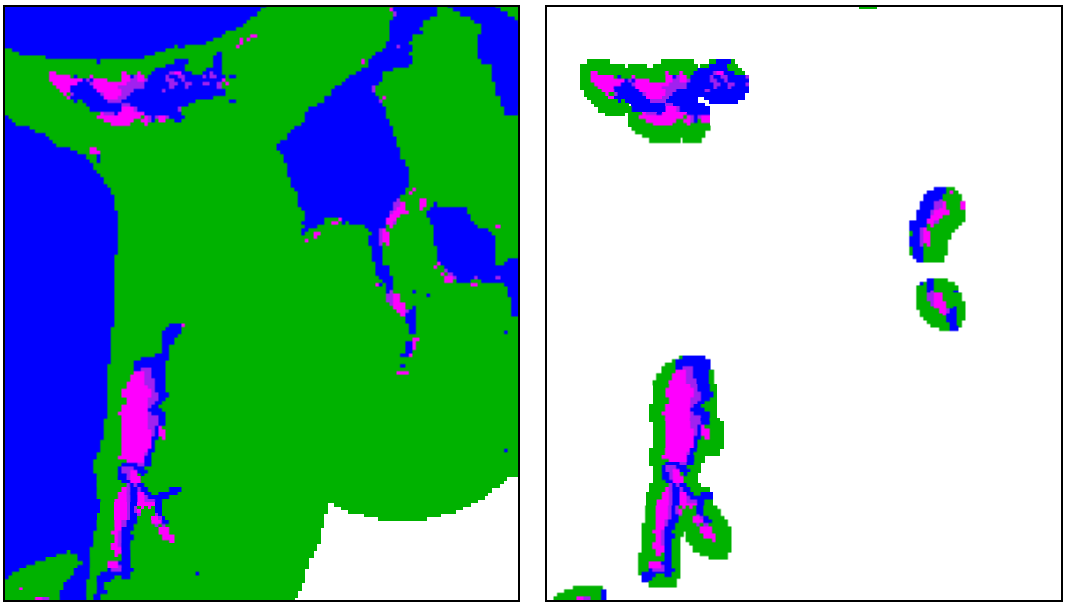

Full classification extent 90-meter buffered classification extent

Figure 10. Examples of a portion of the full Landsat classification and the 90-meter buffered area around classified tidal wetlands.

Table 2. Accuracy assessment of a reduced spatial extent of the September 8, 2002 Landsat classification.

	Reference					
Classified	**Water**	**Low Marsh**	**High Marsh**	**Upland**	**Totals**	**Users Accuracy**
Water	64	8	1	2	75	85.33%
Low Marsh	3	59	12	1	75	78.67%
High Marsh	0	2	69	4	75	92.00%
Upland	0	1	12	62	75	82.67%
Totals	67	70	94	69	300	
Producers Accuracy	95.52%	84.29%	73.40%	89.86%		

Number Correct = 254 out of 300
Overall Accuracy = 84.67%
Overall Kappa Statistic = 0.7956

Table 3. Assessment of the overlap classification.

	8 SEPTEMBER 2002					
31 JULY 2002	**Water**	**Low Marsh**	**High Marsh**	**Upland**	**Totals**	**User's Accuracy**
Water	1,488,673	1,866	839	3,122	1,494,500	99.61%
Low Marsh	444	929	1,540	275	3,188	29.14%
High Marsh	338	788	16,184	3,568	20,878	77.51%
Upland	11,025	952	8,056	509,207	529,240	96.21%
Totals	1,500,480	4,535	26,619	516,172	2,014,993	
Producer's Accuracy	99.21%	20.49%	60.80%	98.65%		

Number of Pixels Agreeing = 2,014,993 out of 2,047,806
Overall Agreement = 98.40%

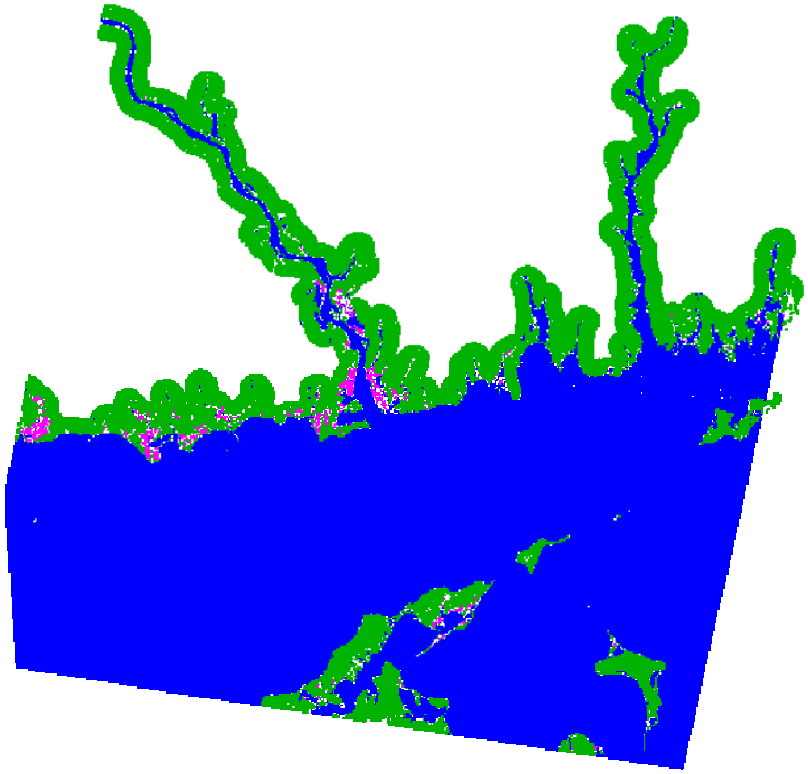

Figure 11. Extent of the overlap classification area between P13/R31 September 8, 2002 Landsat and P12/R31 July 31, 2002 Landsat.

the lowest level of agreement in terms of User's and Producer's accuracy. A considerable amount of this error is between the low and high marsh categories although there is a large amount of low marsh pixels in the September 8, 2002 classified as water in the July 31, 2002 classification. A close up view of the comparison is provided in Figure 12.

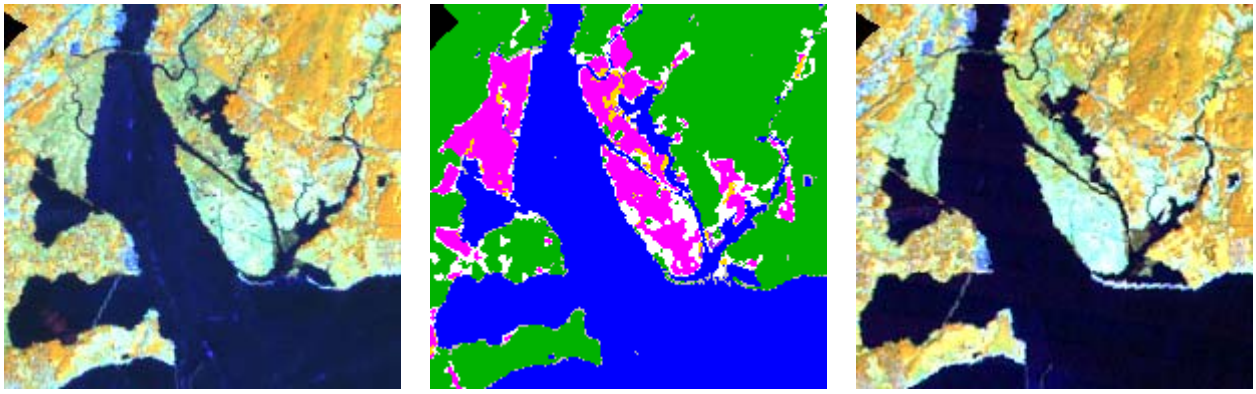

September 8, 2002 Landsat

Classification agreement and disagreement
Blue = water agreement
Purple = low marsh agreement
Magenta = high marsh agreement
Green = upland agreement
White = water/upland to low/high marsh disagreement
Gold = low marsh to high marsh disagreement
Grey = water to upland disagreement

July 31, 2002 Landsat

Figure 12. Example of the comparison of the September 8, 2002 and July 31, 2002 classifications highlighting areas of classification agreement and disagreement.

Analysis of Marshes in the Context of Surrounding Land Cover

Since tidal wetlands occupy a unique niche on the landscape, usually nestled between upland and tidal waters, they are often spatially limited and under pressure on one side from water pollution and sea level rise and on the other side from encroachment, development, and pollution. This portion of the project looked at factors that are likely to influence the potential health of the tidal marshes classified and to identify those marshes most at risk. The basis of this analysis came from a Technical Report on the planning process for the Blackbird-Millington Corridor Conservation Area Plan[4]. The Corridor area includes tidal wetlands and included analysis to assess the health of these wetlands. Planners in the Blackbird-Millington study looked at five indicators of healthy tidal wetlands and waters. These include: the ability to migrate (as indicated by unaltered topography), connectivity to upland habitats (as indicated by natural buffers), natural hydrologic regime (as indicated by the amount of impervious surfacing in the watershed and the extent of ditching and groundwater removal), natural hydroperiod (as indicated by unimpaired tidal exchange), and characteristic ecological community composition, distribution, and vegetation (as indicated by the absence of invasive *Phragmites*). Based on these guidelines, a similar assessment was conducted on the results of the Landsat-based tidal wetland classification of this project, although some of the above measures were not included due to lack of information and this analysis being at a coarser scale. The following sections describe each of the indicators examined.

[4] http://www.dnrec.state.de.us/nhp/information/blackbird.asp (last accessed April 4, 2007)

Connectivity to Upland Habitats: This measure evaluates the existence of natural and built-up upland cover adjacent to identified tidal wetlands. It is assumed that natural vegetation at the edge of tidal wetlands will provide erosion control and wildlife benefits. Therefore, the extent of the connection between the tidal marsh and natural upland areas is vital for the maintenance of the health of tidal marshes. Conversely, built-up areas adjacent to tidal wetlands will negatively impact the wetland by allowing an increase in the amount of fresh, nutrient-rich water running into the marshes and providing suitable habitat for the spread of *Phragmites*. To determine the amount of natural and built-up cover within two buffer zones of 100-meters and 200-meters, the CLEAR CCL[5] land cover from 2002 was used. Any land cover classified as deciduous forest, coniferous forest, non-forested wetland, forested wetland, or tidal wetland in the CCL land cover was considered natural cover. The developed category was used as the built-up cover. Water remained as water, and barren land remained as barren. Buffered areas of 100-meters and 200-meters were identified surrounding each classified tidal marsh from this project and the amount of each of the four land cover types quantified for each marsh. A ranking was then applied to each tidal wetland based on the amount of natural and built-up cover that existing within each of the buffered zones following the rules from the Blackbird-Millington Corridor Conservation Area Plan. Table 4 provides the application of the rankings to each tidal marsh. Figure 13 shows an example of the ranking results for a select few marshes.

Table 4. Indicator rankings based on the amount of natural land cover within 100-mters or 200-meters of classified tidal marshes (colored box represent the color scheme shown for each marsh in Figure 12).

Upland Habitat Connectivity	**Poor (rank 1)**	**Fair (rank 2)**	**Good (rank 3)**	**Very Good (rank 4)**
100-meter buffer (% natural cover)	**<75%**	**75 - 90%**	**90 - 95%**	**>95%**
100-meter buffer (% built-up cover)	**<25%**	**10 – 25%**	**<10%**	
200-meter buffer (% natural cover)	**<50%**	**50 - 80%**	**80 - 90%**	**>90%**
200-meter buffer (% built-up cover)	**<25%**	**10 – 25%**	**<10%**	

Ability to Migrate: The sea level rise zone is the areas of low elevation less then 1-meter above sea level adjacent to the classified tidal wetlands. It is assumed that as sea level continues to rise, the wetlands will require un-altered low elevation areas into which to migrate if the wetlands are unable to keep pace with rising sea level. Without low lying areas suitable for migration, they are at risk of being lost to open water. A 1-meter threshold was selected based on two factors; the 100 year sea level rise prediction of 59 centimeters by the Intergovernmental Panel on Climate Change (2007) and the one-meter vertical resolution of the USGS NED 10-meter digital elevation model. Due to the relative spatial coarseness of the NED DEM, it was felt using any value lower then 1 meter would not yield adequate results.

[5] http://clear.uconn.edu/projects/landscape/index.htm

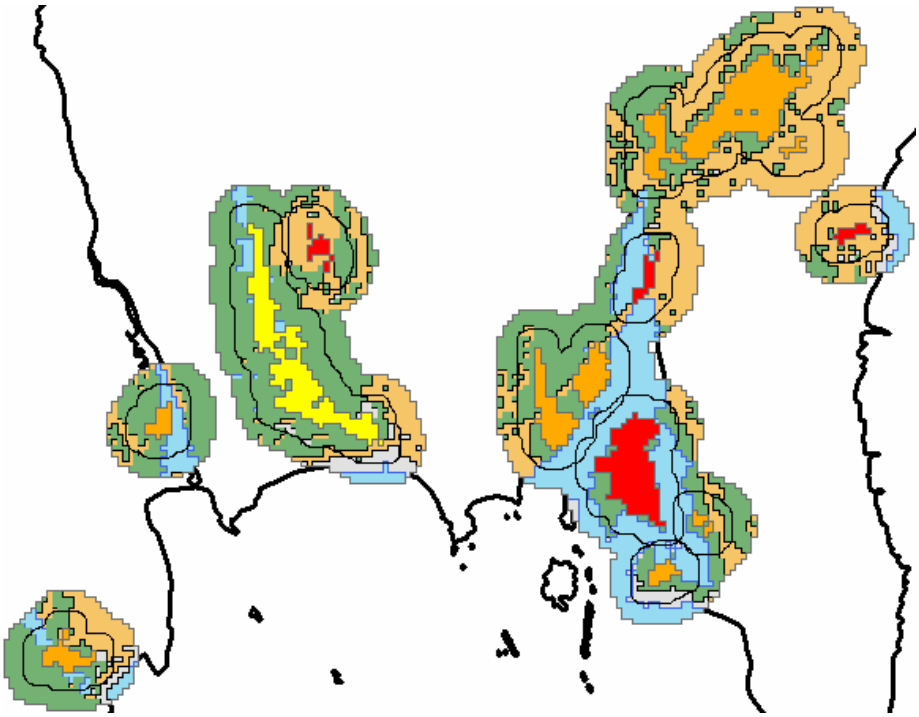

(a) 100-meter buffered area of natural cover (represented by thin black line).

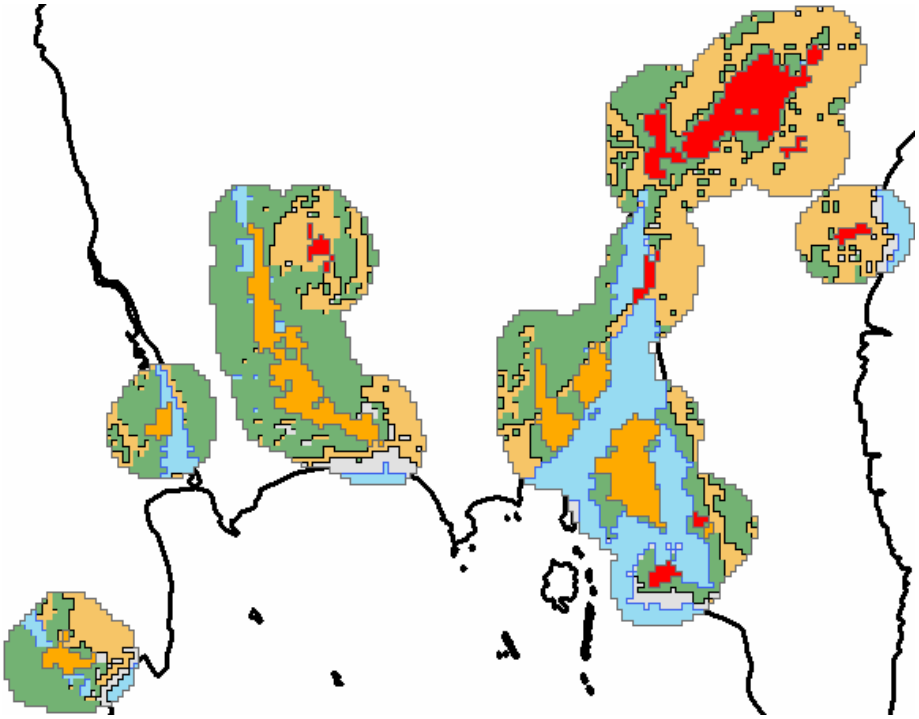

(b) 200-meter buffered area of natural cover

Figure 13. Analysis of adjacent natural land cover to classified tidal marshes within (a) 100-meter and (b) 200-meter buffered areas. The light green areas represent natural land cover, light orange anthropogenic land cover, light blue is water, and gray is barren land.

As it was, very few areas below 1 meter were identified adjacent to tidal wetlands due to the coarseness and errors within the NED DEM data. Once the sea level rise zone was identified, the abundance of built-up land cover was calculated. Table 5 provides the application of the rankings to each tidal marsh based on the percentage of built-up area with the sea level rise zone. Figure 14 shows an example of the ranking results for a select few marshes.

Table 5. Indicator rankings based on the amount of built-up area within the identified sea level rise zone adjacent to classified tidal marshes (colored box represent the color scheme shown for each marsh in Figure 13).

Wetland Migration (sea level rise zone area contains)	**No adjacent low elevation area (rank 0)**	**Poor (rank 1)**	**Fair (rank 2)**	**Good (rank 3)**	**Very Good (rank 4)**
Built-up area	**0**	**> 25%**	**15-25%**	**10-15%**	**< 10%**

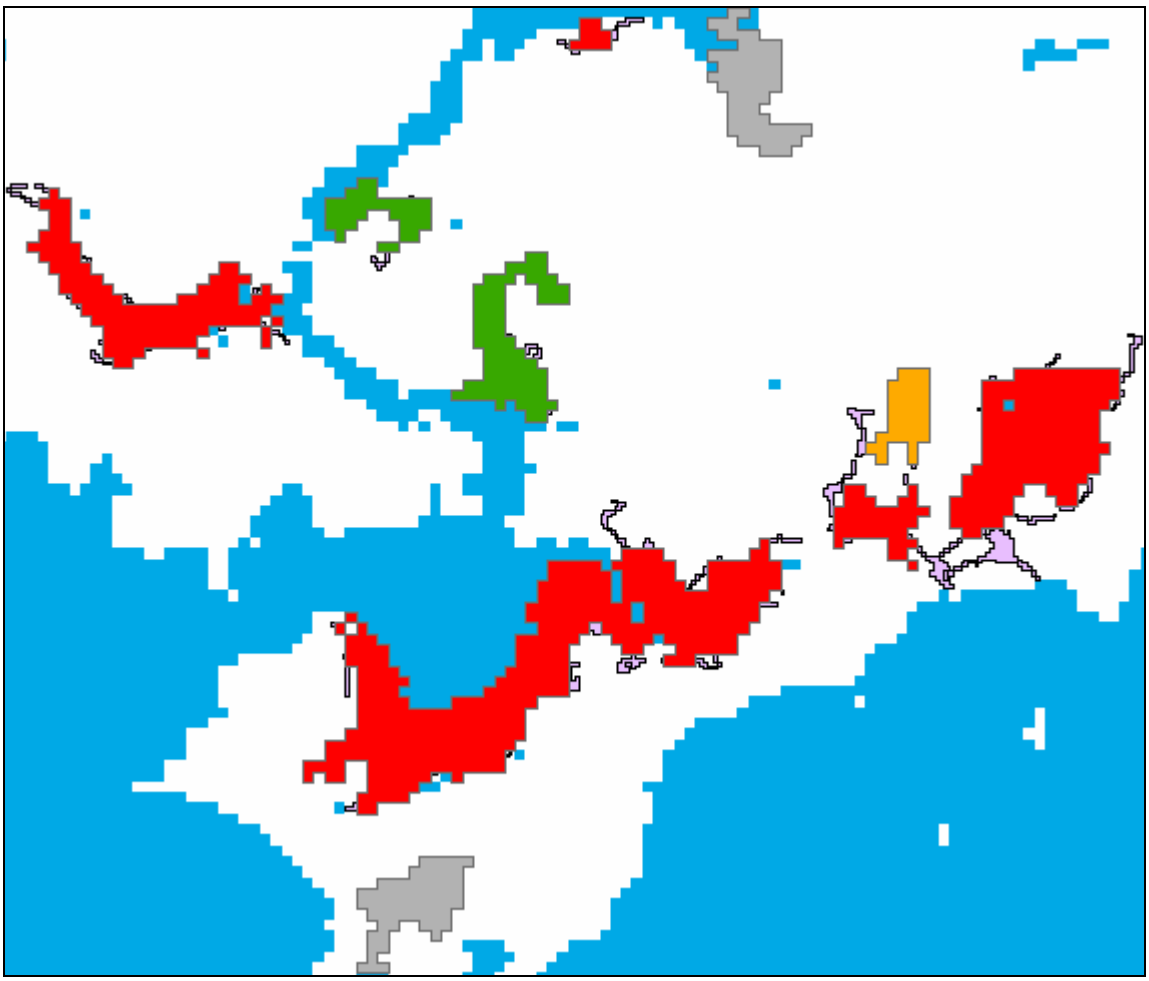

Figure 14. Classified tidal wetlands with adjacent sea level rise zones identified as light purple.

Watershed Impervious Surfaces: This analysis is based on estimates of impervious surfaces for sub-regional watersheds intersecting the classified tidal wetlands, regardless of where the impervious surfaces fall within the watershed. Impervious surfaces will have the tendency to increase the peak volume of water during a rain event, causing increased stream channel erosion, added pollution, local flooding, and decreased base flow available during drought conditions. Likely, the closer impervious surfaces are to the wetland, the greater the impact of that impervious surfaces. But, for this project, if a watershed contains a classified tidal wetland, that wetland is assigned the imperviousness value of the intersecting watershed. Impervious surface estimates were calculated for each sub-regional drainage basin based on the LISS 2002 sub-pixel impervious surface estimation[6]. Table 6 provides the application of the rankings to each tidal marsh based on the percentage of impervious surfaces within the intersecting sub-regional watershed. Figure 15 shows an example of the ranking results for a select few marshes.

Table 6. Indicator rankings based on the amount of impervious surfaces within the intersecting sub-regional watershed (colored box represent the color scheme shown for each marsh in Figure 14).

Impervious Surfaces (area of sub-regional drainage basin covered)	**Poor (rank 1)**	**Fair (rank 2)**	**Good (rank 3)**	**Very Good (rank 4)**
% Impervious Surfaces	**>15%**	**10-15%**	**5-9%**	**<5%**

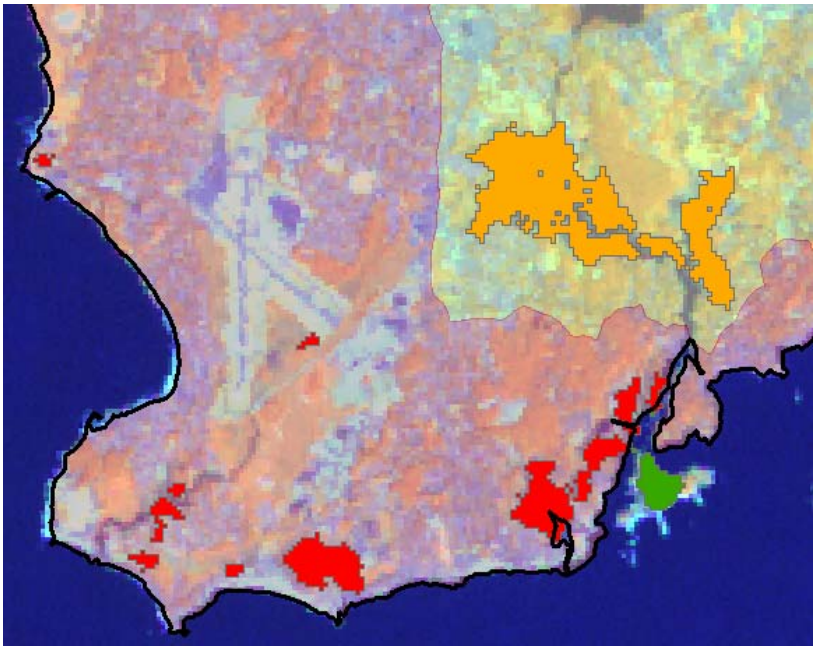

Figure 15. Classified tidal wetlands with intersecting sub-regional watershed imperviousness displayed. Red shaded watersheds have impervious surfaces greater then 25%, yellow shaded watersheds have between 10 and 25% imperviousness.

[6] http://clear.uconn.edu/projects/imperviouslis/project.htm

Final Tidal Wetland Rankings Identifying Potential Health and Sustainability: The results of the rankings for each of the six indicators examined were summed to provide the final ranking values for each classified tidal wetland. Values ranged from five to twenty-one. These were adjusted to a range of 1 (most at risk) to 16 (least at risk). Table 7 identifies the number of tidal wetlands classified falling into each of the ranking categories. Additionally, Figure 16a provides an example of classified tidal marshes and their respective marsh ranking. The rankings were also further condensed into three categories to identify those tidal marshes most at risk (values 1 – 6), moderately at risk (values 7 – 10), and least at risk (values 11-16). These are shown in Figure 16b. While not conclusive, this assessment may provide beneficial information when attempting to identify tidal marshes most at risk to degradation.

Table 7. Marsh rankings and number of marshes contained within each rank value based on the classification of 875 marsh units along Long Island Sound.

Most At Risk		**Moderately At Risk**		**Least At Risk**	
Marsh Rank	Number of Marshes	Marsh Rank	Number of Marshes	Marsh Rank	Number of Marshes
1	13	7	77	11	41
2	42	8	118	12	148
3	58	9	61	13	34
4	46	10	54	14	6
5	75			15	13
6	84			16	3
TOTAL	**318**	**TOTAL**	**310**	**TOTAL**	**245**

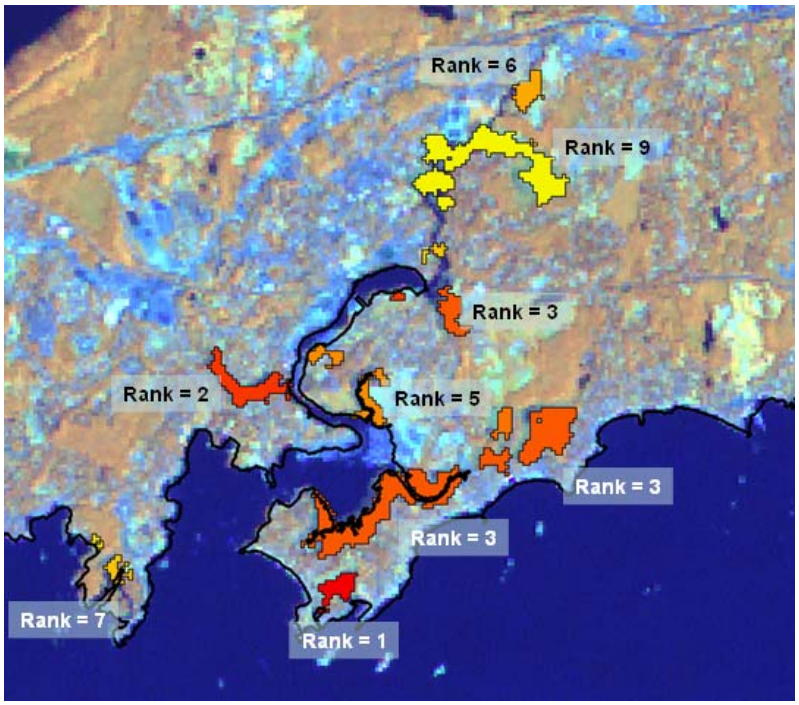

(a) Individual marsh rankings

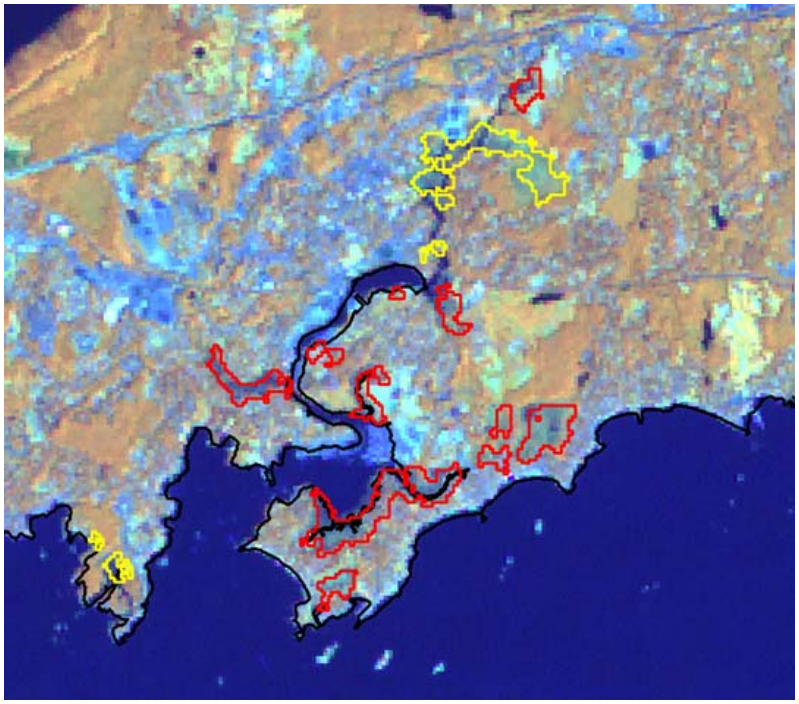

(b) Condensed marsh rankings (marshes outlined in yellow are at moderate risk, marshes outlined in red are at high risk)

Figure 16. Example of the final result of the analysis of upland conditions on the potential health and sustainability of classified tidal wetlands. Image (a) shows the individual marsh rankings whereas image (b) shows the condensed rankings. Red outline identifies the boundary of tidal marshes most at risk, yellow are tidal marshes moderately at risk, and green (not shown) are tidal marshes with least risk. Boundaries are displayed on the September 8, 2002 Landsat ETM image.

Monitoring changes in coastal marshes

A September 28, 1989 Landsat Thematic Mapper image was acquired to compare and assess potential tidal wetland change against the September 8, 2002 ETM image. There are several techniques for conducting change detection. Such methods include comparison of land cover classifications, multidate classification, image differencing/ratioing, vegetation index differencing, principal components analysis and change vector analysis (Singh, 1989). Change detection with spectral remote sensing data is based on the idea that any change in land cover will result in changes in radiance values that are large enough to be detected. One of the problems with this is that radiance value change can be caused by other factors such as differences in atmospheric conditions, differences in sun angle and differences in soil moisture.

To reduce the impact of radiance difference among the two dates of imagery, the September 28, 1989 Landsat TM image was histogram matched to the September 8, 2002 Landsat ETM (Figure 17). Histogram matching is the process of generating a histogram from one image to resemble the histogram of another image. To be most effective, the two images should have similarly shaped histograms and relative dark and light features. Once the histograms are matched, image differencing was performed using the Change Detection module in ERDAS IMAGINE 9.1. This procedure performs a simple subtraction process of a selected band from a T_1 image (September 28, 1989) and T_2 image (September 2, 2002). The near infrared (band 4) band was used for image differencing since it most clearly distinguishes among water, vegetation, and some built-up features. The resulting output is a grey scale image where dark and bright pixels represent areas of reflectance change (likely areas of land cover change) and gray pixels represent areas of little reflectance change (likely areas of no land cover change). The initial results of this analysis did not highlight significant areas of change in the tidal wetlands. To improve the analysis and focus analysis on just the tidal wetlands, image pixels from each image were extracted from just those areas classified as low or high marsh from the 2002 classification. Image differencing was again performed to highlight change in the tidal marshes. The results indicated there was substantial change occurring in the tidal marshes, but the change was due primarily to reflectance change between the images and not related to land cover change, due perhaps to phenological differences, tidal stage, or simply radiometric differences between the two scenes. Figure 18 provides examples of this analysis.

September 28, 1989 Landsat TM histogram matched

September 8, 2002 Landsat ETM

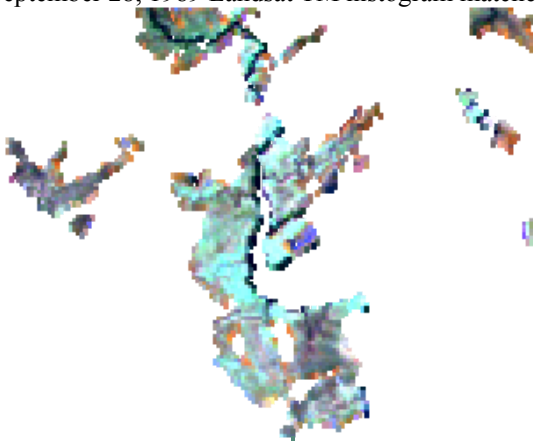

September 28, 1989 Landsat TM
Extraction of tidal wetland areas based on classification of 2002 ETM image.

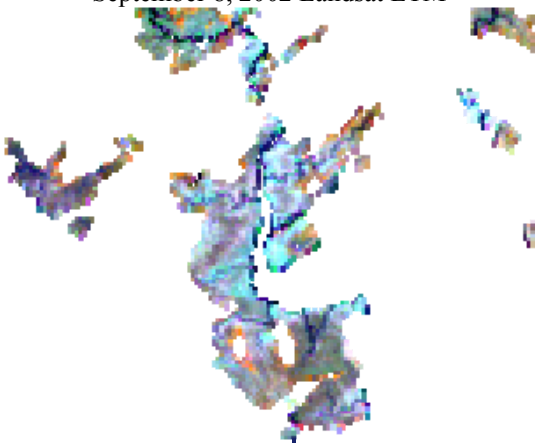

September 8, 2002 Landsat ETM
Extraction of tidal wetland areas based on classification of 2002 ETM image.

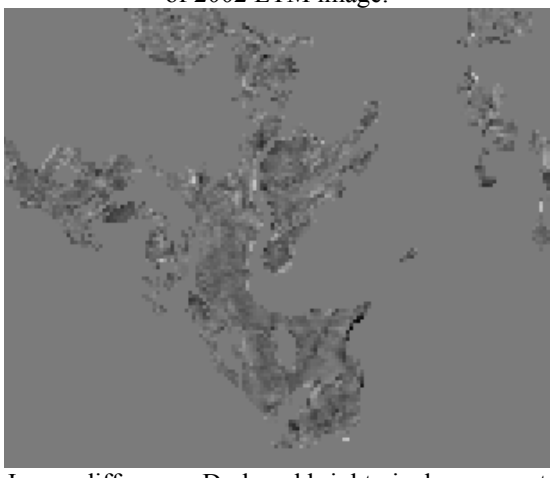

Image difference. Dark and bright pixels represent reflectance change. Gray pixels represent no change

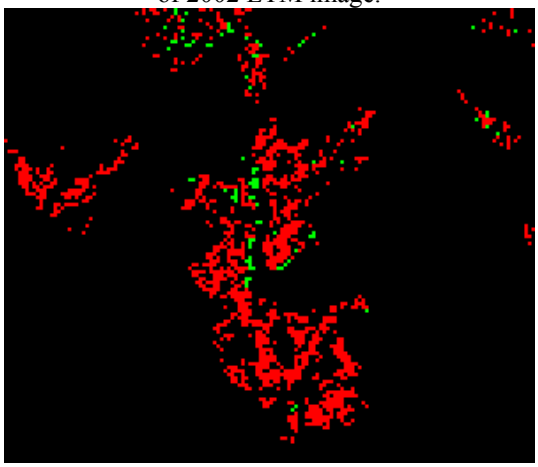

Highlight Change Image. Green areas identify pixels that have a reflectance change of greater then 10 percent

Figure 17. Examples of the histogram matching of the September 28, 1989 Landsat TM image to the September 8, 2002 Landsat ETM image.

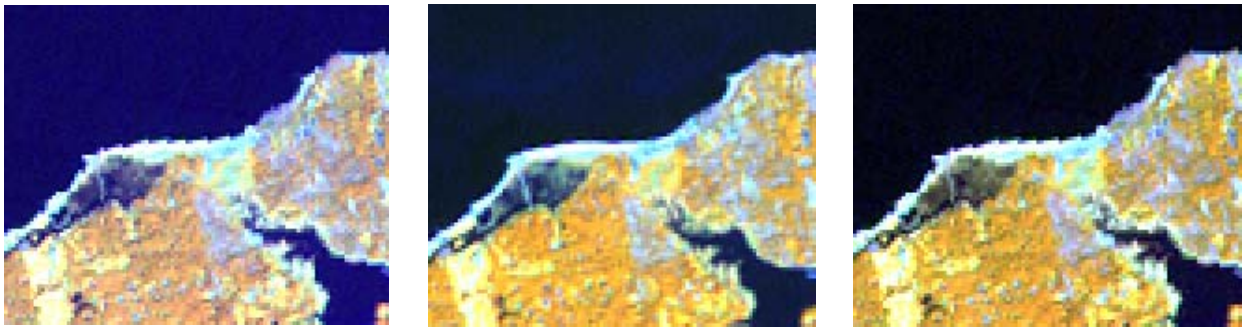

September 28, 1989
Landsat TM

September 8, 2002
Landsat ETM

September 28, 1989
Landsat TM histogram matched to
September 8, 2002 Landsat ETM

Figure 18. Examples of image differencing to highlight areas of land cover change.

Assessment of ASTER imagery

ASTER satellite imagery has better spatial resolution than Landsat (Table 8), and may therefore result in an improved wetland classification. Because ASTER has a smaller area of coverage and is collected much less frequently than Landsat, it was not possible to obtain a consistent set of ASTER imagery to cover the entire Long Island Sound area during the growing season. Some ASTER imagery contemporaneous with the September 8, 2002 Landsat scene was obtained for the western portion of the Sound. A comparison of classification between ASTER and Landsat imagery was therefore possible to assess which sensor would produce a more accurate tidal wetland classification. To perform this assessment, two independent classifications were conducted. Subsets of ASTER and Landsat imagery were selected for the Wheeler Marsh area of Connecticut (Figure 19). The ASTER image was collected on September 9, 2004 whereas the Landsat image was collected on September 8, 2002. Although from different years, the data are from the same portion of the growing season which is critical for comparison.

Table 8. Spatial and spectral characteristics for ASTER and Landsat satellite imagery.

ASTER			LANDSAT ETM		
Band	**Spatial Resolution**	**Spectral Resolution**	**Band**	**Spatial Resolution**	**Spectral Resolution**
	--	--	1	30-meters	Blue 0.45-0.52 um
1	15-meters	Green 0.52-0.60 um	2	30-meters	Green 0.52-0.60 um
2	15-meters	Red 0.63-0.69 um	3	30-meters	Red 0.63-0.69 um
3	15-meters	NIR 0.76-0.86 um	4	30-meters	NIR 0.76-0.90 um
4	30-meters	SWIR 1.60-1.70 um	5	30-meters	SWIR 1.55-1.75 um
5	30-meters	SWIR 2.145-2.185 um	6	60-meters	Thermal 10.4-12.5 um
6	30-meters	SWIR 2.185-2.225 um	7	30-meters	SWIR 2.08-2.35 um
7	30-meters	SWIR 2.235-2.285 um		--	--
8	30-meters	SWIR 2.295-2.365 um		--	--
9	30-meters	SWIR 2.360-2.430 um		--	--

ASTER Satellite Image
September 9, 2004
Near-infrared, red, green bands displayed

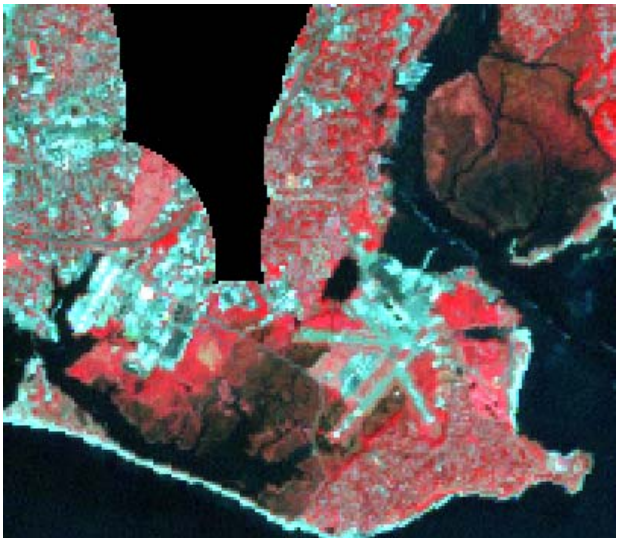

Landsat ETM Satellite Image
September 8, 2002
Near-infrared, red, green bands displayed

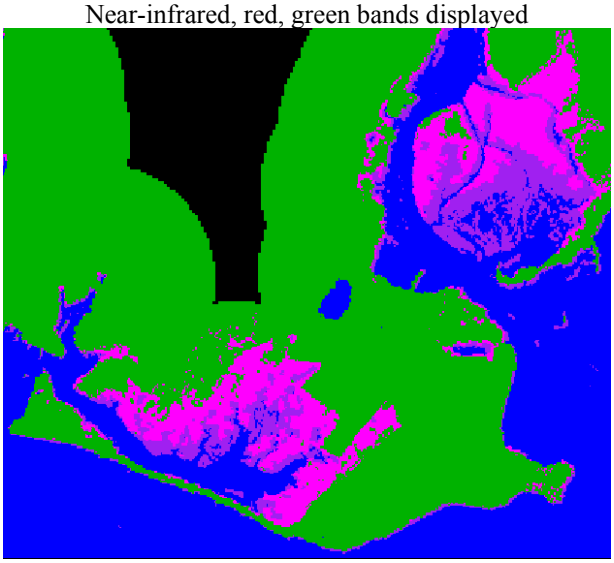

Classification from ASTER imagery

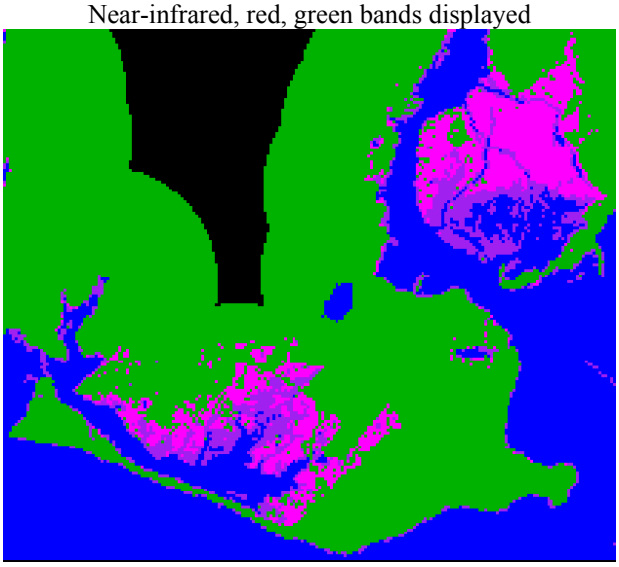

Classification from Landsat imagery

Figure 19. Comparison of the classification of tidal wetlands from both ASTER and Landsat ETM satellite imagery (water is blue, upland is green, high coastal marsh is magenta, low coastal marsh is purple).

To classify each image, the NLCD Mapping Tools created through the National Land Cover Dataset program were used generate training information and apply the classification. Several training pixels were selected that represent various land cover features within each image. These include: dark, medium, and bright built-up features, grass, forest, water, low marsh and high marsh features. The same training point was used for each image to maintain consistency. These training data were applied to each image from which appropriate files were generated to apply to See5, a data mining tool. See5 was applied to derive an appropriate classification tree (see Figure 20). The classification tree was then applied to the image data to derive a final classification. The classes were recoded into water, low marsh, high marsh, and upland. Additionally, the upland area was edited to remove misclassified low and high marsh from the upland areas.

Classification Tree Derived from ASTER Image

```
band05 <= 9: Water (347)
band05 > 9:
:...band06 <= 26:
    :...band04 <= 24:
    :   :...band07 <= 16: Low Marsh (50)
    :   :   band07 > 16: Developed1 (81)
    :   band04 > 24:
    :   :...band03 > 84: Forest (19)
    :       band03 <= 84:
    :       :...band08 <= 18: High Marsh (242)
    :           band08 > 18:
    :           :...band08 <= 20: Developed4 (3)
    :               band08 > 20: Developed1 (5)
    band06 > 26:
    :...band03 > 91:
        :...band01 <= 152: Grass2 (69)
        :   band01 > 152: Developed3 (9)
        band03 <= 91:
        :...band03 <= 57: Developed2 (69/3)
            band03 > 57:
            :...band01 <= 88: Grass1 (37/1)
                band01 > 88:
                :...band08 <= 27: Developed4 (12/3)
                    band08 > 27: Barren (25)
```

Classification Tree Derived from Landsat Image

```
band04 <= 31:
:...band04 <= 13: Water (97)
:   band04 > 13:
:   :...band06 <= 140: Low Marsh (31)
:       band06 > 140: Developed1 (35)
band04 > 31:
:...band01 <= 70:
    :...band04 <= 72: High Marsh (89)
    :   band04 > 72: Forest (15/2)
    band01 > 70:
    :...band05 <= 85:
        :...band07 <= 46: Developed4 (12/2)
        :   band07 > 46:
        :   :...band01 <= 87: Developed4 (4)
        :       band01 > 87: Developed2 (29/2)
        band05 > 85:
        :...band04 <= 77:
            :...band02 <= 65: Grass1 (17)
            :   band02 > 65: Barren (21/3)
            band04 > 77:
            :...band03 <= 112: Grass2 (37/2)
                band03 > 112: Developed3 (8)
```

Figure 20. Resulting classification trees from both the ASTER and Landsat images based on similar training data. Band numbers correspond to bands listed in Table 8.

Accuracy assessment was performed on 150 stratified random sample of points. The same set of points was used for each classification. Points were compared against the ASTER and Landsat imagery and high resolution ADS40 imagery which served as the reference data. Reference information was compared with the classified information for each sample point to produce an error matrix to calculate overall, user's and producer's accuracy. The results are reported in Table 9 and Table 10. Both classifications have similar overall accuracies with the Landsat classification producing a slightly higher overall classification accuracy. It was expected the ASTER image would have produced the better result given its improved spatial resolution in three bands and larger number of spectral bands used in the classification. These results indicate that the Landsat ETM sensor, with its larger areal coverage, would be a more suitable candidate for conducting a classification compared to the ASTER sensor. Further, the 15-meter panchromatic band on Landsat ETM can be used to sharpen the 30-meter multispectral data yielding a fused 15-meter multispectral image. Data fusion algorithms will be examined in future research.

Table 9. ASTER classification accuracy.

		Reference					
		Water	Low M.	High M.	Upland	TOTAL	User's Accuracy
Classified	Water	43	0	0	0	43	100.00%
	Low M.	4	14	0	2	20	70.00%
	High M.	0	3	15	5	23	65.22%
	Upland	0	0	0	64	64	100.00%
	TOTAL	47	17	15	71	***150***	
	Producer's Accuracy	91.49%	82.35%	100.00%	90.14%		***Overall Acc. 90.67%***

Table 10. Landsat classification accuracy.

		Reference					
		Water	Low M.	High M.	Upland	TOTAL	User's Accuracy
Classified	Water	45	0	0	0	45	100.00%
	Low M.	1	10	0	2	13	76.92%
	High M.	0	3	16	2	21	76.19%
	Upland	0	2	1	68	71	95.77%
	TOTAL	46	15	17	72	***150***	
	Producer's Accuracy	97.83%	66.67%	94.12%	94.44%		***Overall Acc. 92.67%***

Task 2. Identification of vegetative species within marshes

The major goal here to use high-resolution image data to identify specific marsh vegetative species in the marshes. This required knowledge of the spectral reflectance characteristics of individual species, which change throughout the growing season. To address this, we collected reflectance spectra of major marsh species using a spectroradiometer in the field over two entire growing seasons. These data were then compared to QuickBird satellite data (2.44 m/pixel, 4 bands: blue, green, red, NIR). Field measurements were collected for the marsh species *P. australis*, *Typha spp.*, *S. patens* and *S. alterniflora*, where present at five marshes during the 2004 growing season: Wheeler Marsh, Flax Pond, Barn Island Marsh, Ragged Rock Creek Marsh, and Chapman Pond. This experience guided collection of data for the 2005 season, which included biweekly measurements at a single site, Ragged Rock Creek Marsh. This repeatability was necessary to capture changes in plant phenology throughout the growing season. Ragged Rock was also accessible without a boat and located at the mouth of the CT River where repeated sets of QuickBird satellite data were available. Reflectance spectra were examined to determine when during the year species were most distinguishable from one another. These results formed the basis for a set of rules that were applied to the classification of QuickBird data for Ragged Rock Creek Marsh.

Collection of in situ spectral measurements of *P. australis* and other marsh species at other CT marshes and production of a marsh vegetation spectral library

Reflectance spectra were obtained of dominant marshes species *in situ* using an ASD Fieldspec FR spectroradiometer (Analytical Spectral Devices, Boulder, CO) with a wavelength range of 350-2500 nm, a sampling interval of 1.4 nm between 350-1000 nm and 2 nm between 1000-2500 nm, and a spectral resolution of 3 nm between 350-1000 nm and 10 nm between 1000-2500 nm. The spectrometer is equipped with a 1 m long fiber optic sensor with a 25˚ field of view. Spectra were collected by positioning the fiber optic sensor ~nadir within 1 m of the species canopy by hand. Late in the season, the height of *Phragmites* prohibited a nadir view and canopy spectra were collected at an oblique angle. Individual spectral measurements were an average of 5 scans and each canopy was generally sampled 10 or more times. Reflectance spectra were normalized to a white Spectralon® (sintered Halon) panel.

Example reflectance spectra of marsh species at Ragged Rock Creek Marsh are shown in Figure 21. The shape of the reflectance spectra of each plant species is broadly similar, including the following absorptions typical of healthy photosynthesizing vascular plants (*e.g.* Mimuro and Katoh, 1991): 430 nm (Chl *a*), 448 nm (Chl *b*, carotenoids), 471 nm (carotenoids), 642 nm (Chl *b*), 662 and 680 nm (Chl *a*), the green peak at 550 nm and strong reflectance in the NIR at approximately 800 nm (Figure 21). At the beginning of the growing season, each spectrum shows expected increases in the strength of the absorptions at approximately 450 nm and 680 nm due to chlorophylls and carotenoids within the leaves and an increase in NIR reflectance due to leaf biomass. This trend continues in each species until the onset of senescence (Figure 21a). Comparison of the spectra of individual species on each sampling date shows that the magnitude and shape of the spectra differ qualitatively (Figure 21b), which is a function of each species' chemistry, biomass and phenological cycle.

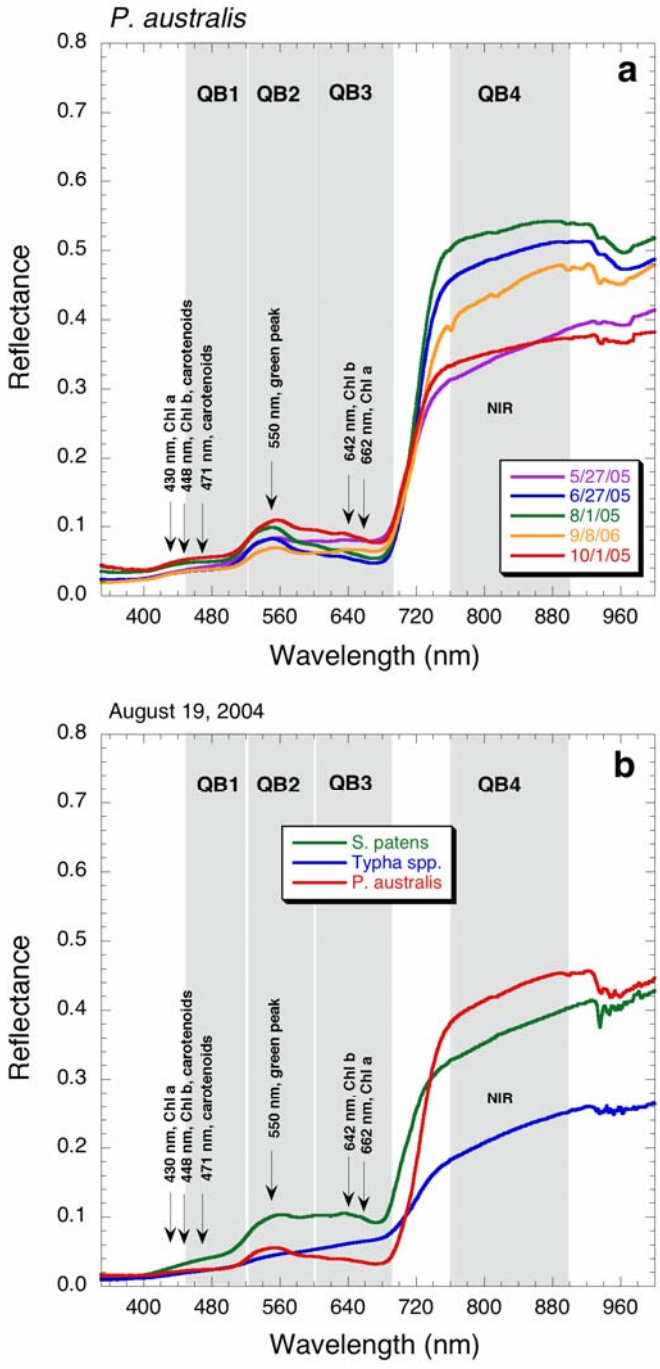

Figure 21. Example reflectance spectra of dominant plant species in Ragged Rock Creek marsh, QuickBird band positions and absorptions due to plant pigments are indicated. (a) P. australis throughout the 2005 growing season. (b) Major species on a single day.

To relate spectral variability to the QuickBird data, reflectance spectra of each species taken during both field seasons were averaged over each QuickBird band (Figure 21); QuickBird band ratios were then calculated and plotted in Figure 21. The spectral behavior is broadly consistent over the two growing seasons. Trends of NDVI and the NIR/red ratios mimic each other, where the NIR/red ratio provides greater separability amongst the individual points (Figure 22a and 22b). All species show a rise in these indices at approximately day 160 (early June) corresponding with the green-up phase of plant growth and a subsequent decline in the indices corresponding to senescence. The behavior of the seasonal variation in each index varies with plant species: *S. patens* and *P. australis* reach peak values at day 200 and *Typha spp.* at day 170. *Typha spp.* NDVI and NIR/red values are generally higher than the other species near the time of its peak (mid to late June), while *P. australis* values exceed the other species in mid August through early September.

The seasonal pattern of the QuickBird green/blue ratio of *S. patens* is distinct from the other two species (Figure 22c). Values of this ratio are similar for each species at the beginning of the season, but *S. patens* rises to a peak value near day 200 (mid July). The absolute value for *S. patens* is twice that of *Typha spp.* and *P. australis* from early June through early August.

The general seasonal pattern of the QuickBird red/green ratio for all species shows an initial decline from approximately day 140 to day 180 (late May – late June) and then an increase (Figure 22d). *S. patens* values in this index are lower than the other two species over days 165 to 225 (mid June – early August). *Typha spp.* values exceed those of the other species from mid-July onward.

The general seasonal pattern of the QuickBird NIR/green ratio for all species shows an increase in the middle portion of the growing season and decline at the end (Figure 22e). *S. patens* values in this index are consistently lower than the other two species throughout the year. Values for *Typha spp.* are higher than and separable from the other two species in mid to late June. Spectral index values for *P. australis* are higher than and separable from the other two species in late August – early September.

Of the five simple band ratios calculated from the field reflectance spectra, four were determined to be most useful in identifying at least one major plant community: for *P. australis*, the NIR/red ratio on September 8, 2006, for *S. patens*, the green/blue ratio on July 14, 2004, and for *Typha spp.*, the red/green ratio on August 12, 2005 and the NIR/green ratio on June 15, 2004 (Figure 22). These dates both show the greatest spectral separability between individual species and best correspond with the dates (month, day) of the QuickBird images available for classification

The phenological trends seen here can vary as a function of plant vigor, which may depend on changes in salinity, weather, predation or disturbance. That these trends are consistent over two years suggests that these rules may have broader spatial and temporal application, but are perhaps best limited to regions of consistent climate.

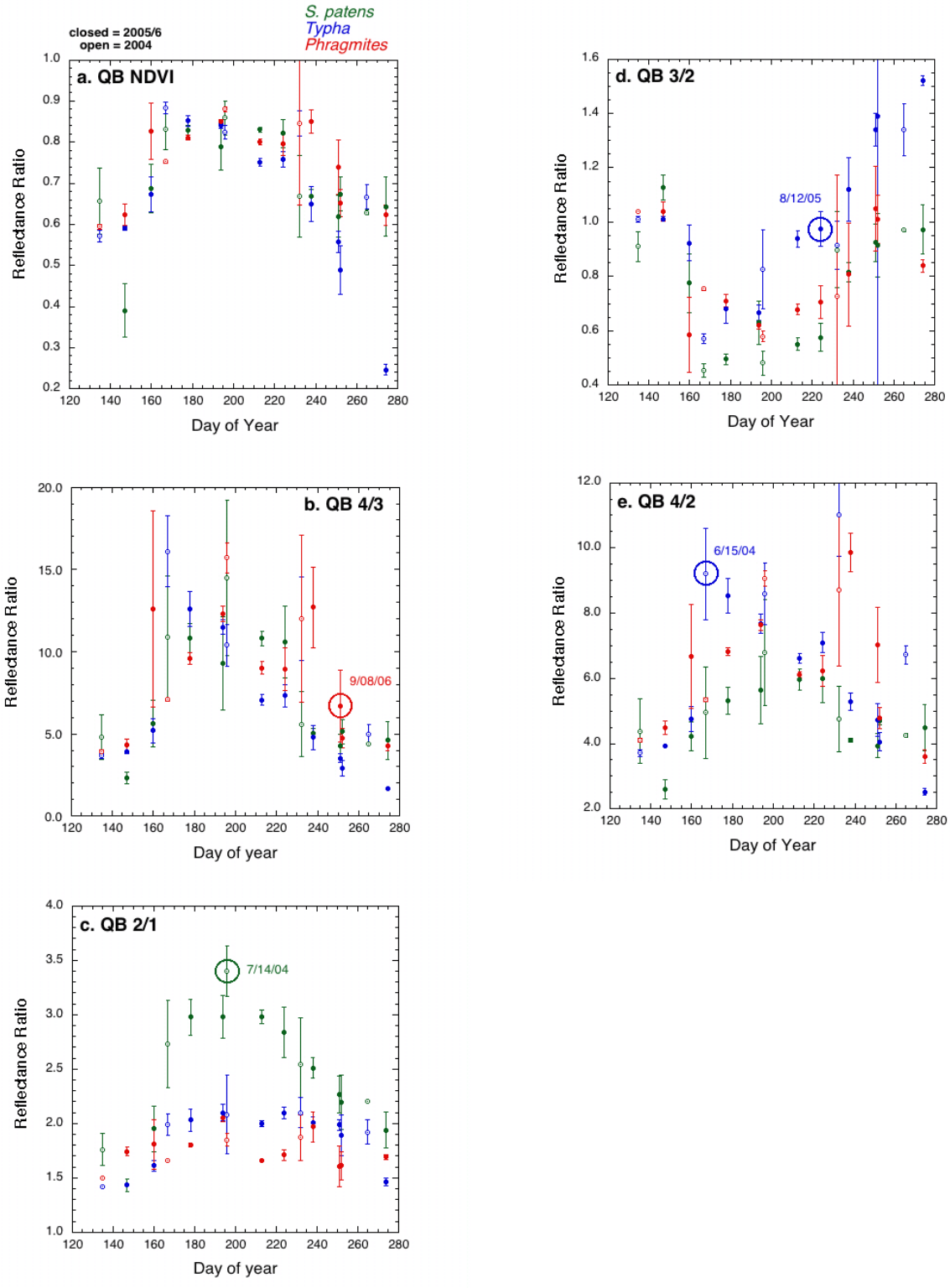

Figure 22. Field reflectance data recalculated as QB bands for the dominant species over the 2004 - 2006 growing seasons. Error bars are one standard deviation. Circles refer to relationships utilized in the classification process.

High Resolution Image Classification

High Resolution Image Data Collection The original research plan called for the use of QuickBird satellite imagery to classify the dominant wetland plants at five select tidal wetlands (Flax Pond, Wheeler Marsh, Great Island, Chapman Pond, and Barn Island). Requests were submitted to DigitalGlobe for the acquisition of image data for each of these sites beginning in 2004 and continuing through the 2005 and 2006 growing seasons (July through September). Due to atmospheric conditions and competing requests for data, QuickBird data were ultimately only acquired at three of the five sites (see Table 11). As such, other high resolution image data were acquired from various sensors and classified to produce tidal marsh classifications. Examples of these are provided in Figure 23.

Table 9. Dates of high spatial resolution image data collected for each of the five study marshes.

	TIDAL WETLAND				
SENSOR	**Wheeler Marsh**	**Chapman Pond**	**Mouth of Connecticut River (Great Island Marsh)**	**Barn Island Marsh**	**Flax Pond**
QuickBird		31 Jul 2003	8 Jul 2003	7 Sept 2004	
		10 Jul 2005	27 May 2004	28 Sept 2005	
			2 Jul 2004		
			20 Jul 2004		
			12 Sep 2004		
			2 Jun 2005		
			17 Jun 2005		
			23 Jul 2005		
			31 Jul 2006		
			13 Aug 2006		
			6 Nov 2006		
ADS40	20 Sep 2004	20 Sep 2004	20 Sep 2004	20 Sep 2004	
John Deere Agri-Services	18 Sep 2006	21 Sep 2006	21 Sep 2006	21 Sep 2006	18 Sep 2006

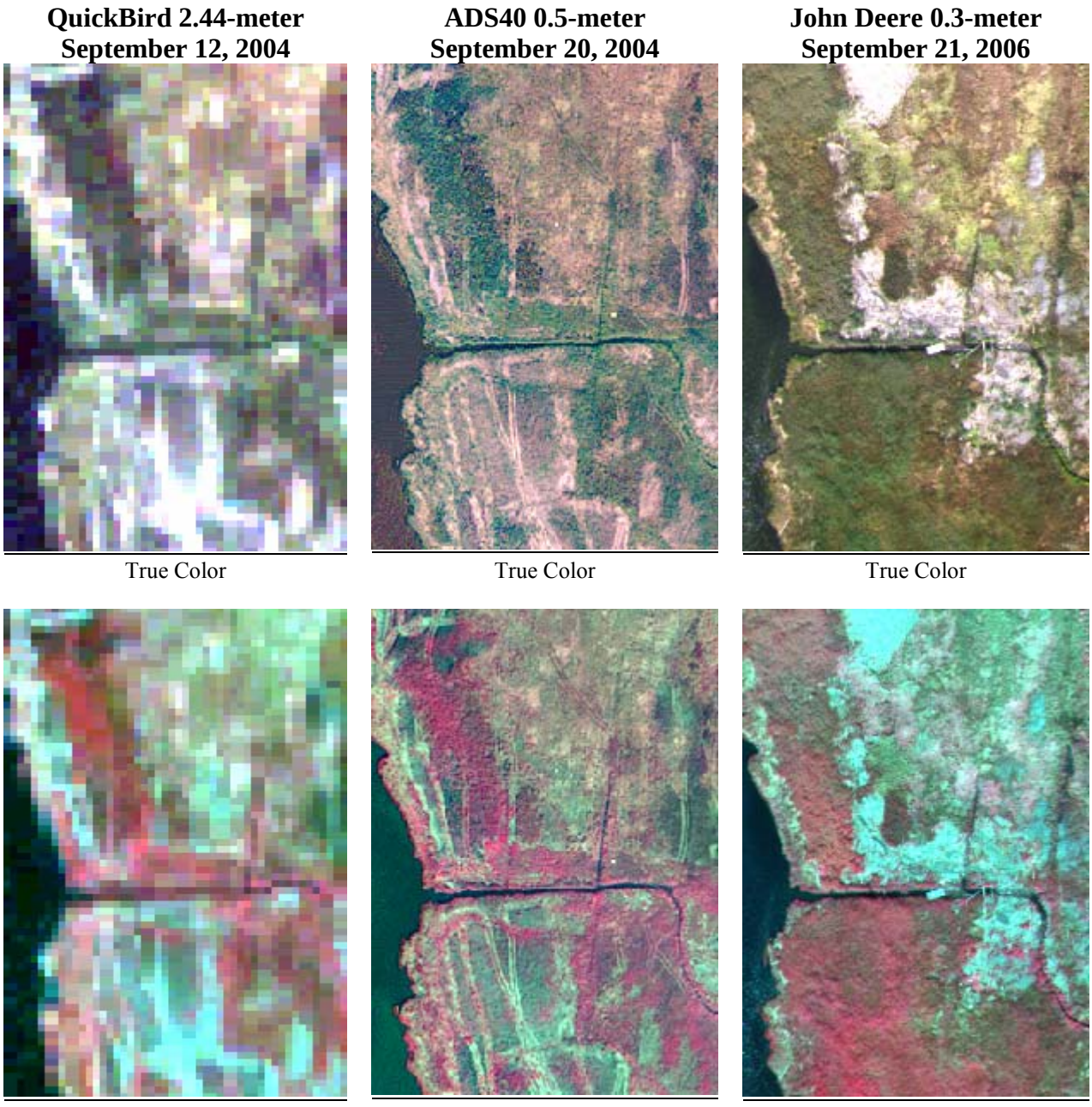

Figure 23. Examples of true color and false color imagery covering the same tidal marsh area from the QuickBird, ADS40, and John Deere Agri-Services sensors. Comparing the QuickBird and ADS40 imagery (from 2004) with the John Deere image (from 2006), the impact of the *Phragmites* control programs where *Phragmites* has been removed and the area treated is noticeable (bright areas in the images).

Ragged Rock Creek Marsh: Classification of the Ragged Rock Creek Marsh, located at the confluence of the Connecticut River with Long Island Sound, was conducted using the eCognition image analysis software (Benz *et al*., 2004). eCognition allows for a variety of image and other data types to be added as input layers to a project file. For this project, input data consisted of individual QuickBird bands from a single date, multiple date band ratios, and

LiDAR top of canopy information**.** LiDAR stands for Light Detection And Ranging and is a technology that uses lasers mounted in an aircraft to measure accurately the elevation of the ground and/or height of canopy. The LiDAR data were collected through another project for the central Connecticut coast area which included the Ragged Rock Creek Marsh area. Together, these data were segmented into image objects which are contiguous pixels that are grouped together into homogeneous polygon features. Each band or layer in the eCognition project was weighted to control how much it contributed to the segmentation (Table 12). The relative size of each object is determined by the scale parameter. In this study, a scale parameter of 20 was found to be the optimum size to identify best the plant communities. Additionally, spectral and spatial parameters were set to contribute 70 percent and 30 percent, respectively to the segment boundary determination. The result is a segmented image consisting of objects, each of which is treated as a single entity. This is in contrast to per-pixel classifiers where each pixel is treated independently of all others, including its neighbors.

Table 12. QuickBird band ratios used for image segmentation. The values indicate the weight applied in eCognition during image segmentation. The July 20, 2004 2:1 ratio is the only one to not have a weight of 0.5 due to the inclusion of the raw Quickbird bands from this date.

Image Date	**Image Weights**					
	Band 2 / Band 1	Band 3 / Band 2	Band 4 / Band 2	Band 4 / Band 3	Raw Bands 1, 2, 3, 4	LiDAR
June 17, 2005	-	-	0.5	0.5	-	-
July 2, 2004	0.5	0.5	0.5	-	-	-
July 20, 2004	0	-	-	-	Bands 1, 2, 3 = 0.8 Band 4 = 1.0	-
August 13, 2006	0.5	0.5	0.5	0.5	-	-
September 12, 2004	0.5	0.5	-	0.5	-	
October 8, 2004	-	-	-	-	-	1.0

Classification in eCognition uses training samples and/or rules. The characteristics of the field spectra (Figure 22) guided the creation of image rules in eCognition (Figure 24). Of the five simple band ratios calculated from the field reflectance spectra, four were determined to be most useful in identifying at least one major plant community from all others on the radiometry rule graphs (Figure 22). The four band ratios (NIR/red, NIR/green, red/green, green/blue) were calculated for the five QuickBird images using image ratio models in Leica Geosystems' ERDAS IMAGINE; the radiometry rules identified that 14 of these band ratio images could potentially be beneficial in classification by contributing to the separation of plant classes. A polygon of the Ragged Rock Creek marsh was created to subset each band ratio image to eliminate variability from non-marsh features such as houses, trees and lawns. One raw QuickBird image was also added to separate water from vegetated areas. The LiDAR dataset was the final addition to the eCognition project. One third of the field points were randomly selected to help guide the classification and the remaining two thirds were reserved for accuracy assessment. Built-in eCognition tools also helped determined the final classification rules and quantitative thresholds (Figure 24).

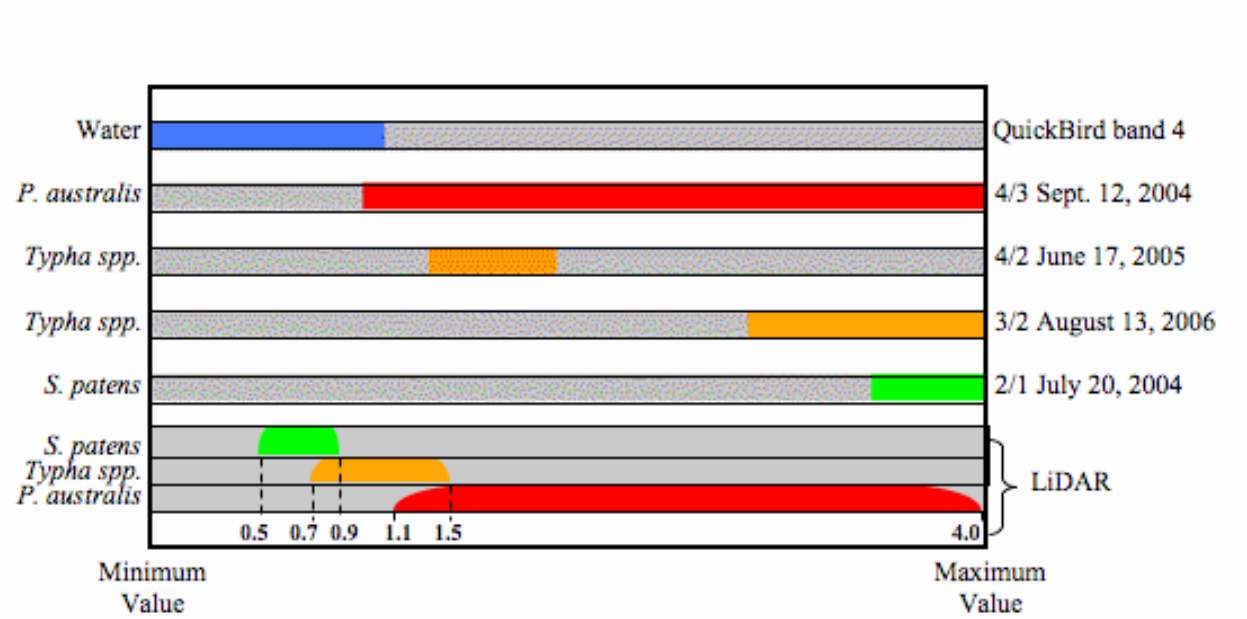

Figure 24. Knowledge-based rules implemented in eCognition for classification of image objects. High values of the September 12, 2004 NIR/red ratio and high values of LiDAR were used to classify P. australis segments. Middle values of June 17, 2005 NIR/green band ratio, high values of the August 13, 2006 red/green band ratio and middle heights of LiDAR identified *Typha spp*. objects. High values of the July 20, 2004 green/blue band ratio and low values of the LiDAR height data determined *S. patens* objects.

QuickBird classification results are displayed in Figure 25. Qualitatively, the classification identifies contiguous areas of *P. australis*, *Typha spp.*, and *S. patens*. The distribution of these classes is broadly consistent with field observations, for example, the correlation of *P. australis* and anticorrelation of *S. patens* with creeks and ditches. The classification confirms that the portion of Ragged Rock Creek marsh surveyed is dominated by the three species under study, where *Typha spp.* and *P. australis,* comprise 34% (44.3 hectares) and 23% (30.5 hectares) respectively, *S. patens* covers 21% (27.8 hectares), and other species cover 22% (28.3 hectares) of the Ragged Rock Creek marsh.

An accuracy assessment of the classification results was performed where each validation point was assigned to a dominant class (Table 13). The overall accuracy was 66.8% with a *kappa* coefficient of 0.56. *P. australis* has the highest user's accuracy (87.0%) and a high producer's accuracy (76.9%). *Typha spp.* has the lowest user's accuracy (59.1%) but the highest producer's accuracy (88.3%) indicating a misclassification of other/mixed reference points as *Typha spp. S. patens* has a similar over classification with 32 points being classified as *S. patens* but being labeled other/mix in the validation dataset. The result is 62% user's accuracy for *S. patens* and a 79.2% producer's accuracy.

Although great care was taken in assigning each point to a single dominant class, the assignment does not mimic real conditions on the marsh. Few plots consisted of a single species and in most cases two or more species contributed to a shared co-dominance. For example, of the 32 points

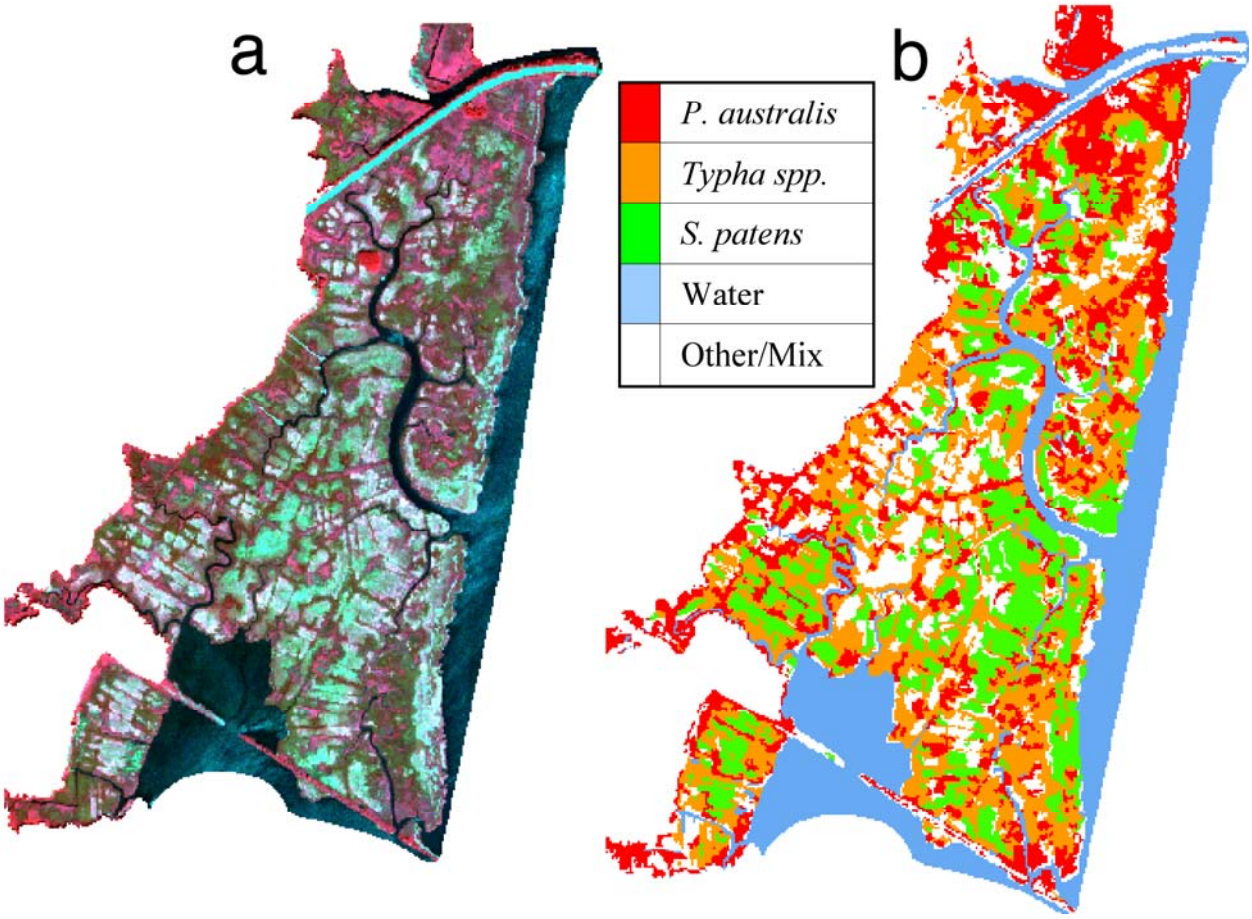

Figure 25. (a) July 20, 2004 QuickBird 4-2-1 image. (b) Classification result.

Table 13. Error matrix for QuickBird classification. Reference data indicate dominant species..

Classified Data	**Reference Field Data**					
Class	*P. australis*	*Typha sp.*	*S. patens*	Other/Mix	**Total**	**Users**
P. australis	60	0	0	9	**69**	87.0%
Typha spp.	13	91	8	42	**154**	59.1%
S. patens	0	3	57	32	**92**	62.0%
Other/Mix	5	9	7	49	**70**	70.0%
Total	**78**	**103**	**72**	**133**	**385**	
Producers	76.9%	88.3%	79.2%	37.1%		
Overall	**66.8%**					
Kappa	0.56					

classified as *S. patens* but labeled other/mix in the reference set, 25 contained some *S. patens* and 17 of the points had a higher percent cover of *S. patens* than any other species. Two of the original 14 dominance classes were species mixes: *P. australis* with *Typha spp.* and *S. Patens* with *Eleocharis spp.* In the six generalized dominance classes, these mixed class points were included in the other/mix class. Another significant factor is the weighting included in the classification. The weighting was necessary to account for the species that have a greater likelihood of being part of the upper canopy as tall, dense species often covering and hiding the

low-growing species. This could result in a point with a very low percentage of *P. australis* and a high percentage of *S. patens* being labeled as *P. australis*-dominant. For example, the three points in the accuracy table classified as *S. patens* but identified as *Typha spp.* all contained *S. patens*.

Because of the difficulty in assigning continuous and complex floristic data to one single class, the accuracy table was re-calculated where the validation data are defined by the presence of the named species (Table 14). This results in an increase in overall accuracy to 82.9% (*kappa* coefficient = 0.77) as well as producer's and user's accuracies in each category. Seven of the nine points classified as *P. australis* but labeled other/mixed, contained some *P. australis*. Although all three species classes show a slight improvement in producer's accuracy with *P. australis* going from 76.9% to 82.7%, *Typha spp.* changing from 88.3% to 92.9% and *S. patens* changing from 79.2% to 85.9%, the greatest improvement in producer's accuracy occur in the other/mix class. In this presence/absence accuracy table, reference points were moved out of the other/mix class and into the appropriate species class, leaving the other/mix class containing points that did not contain any *P. australis, Typha spp.* or *S. patens*. In other words, the other/mix class more accurately represents other species.

Table 14. Error matrix for QuickBird classification. Reference data indicate presence of species.

Classified Data	**Reference Field Data**					
Class	*P. australis*	*Typha sp.*	*S. patens*	Other/Mix	**Total**	**Users**
P. australis	67	0	0	2	**69**	95.1%
Typha spp.	9	118	7	20	**154**	76.6%
S. patens	0	0	85	7	**92**	92.4%
Other/Mix	5	9	7	49	**70**	70.0%
Total	**81**	**127**	**99**	**78**	**385**	
Producers	82.7%	92.9%	85.9%	62.8%		
Overall	**82.9%**					
Kappa	0.77					

Barn Island Marsh

An object-based classification was applied to the QuickBird imagery acquired 28 September 2005. QuickBird data collected for the Barn Island study area were acquired from DigitalGlobe as a resolution enhanced product with 60-centimeter resolution (Figure 26a and 26b). eCognition was used to perform a hierarchical segmentation, the coarser level of which was used for separating water, marsh, and other, and the finer level being used for discriminating among marsh plant species and associations. Two other data layers were used in the segmentation and classification of the QuickBird data: the normalized difference vegetation index[7] (NDVI) (Figure 26c) and top-of-canopy height data, referred to as a Digital Surface Model (DSM), derived from ADS40 digital aerial imagery collected of the coast area of Connecticut in September 2004 (Figure 26d). The latter was super-sampled from its original 2m resolution to 60cm and further geometrically registered to the QuickBird data.

[7] NDVI = (NIR-Red)/(NIR+Red)

(a) QuickBird image the Barn Island Salt Marsh. Bands 3, 2, and 1. Acquired 28 September 2005.

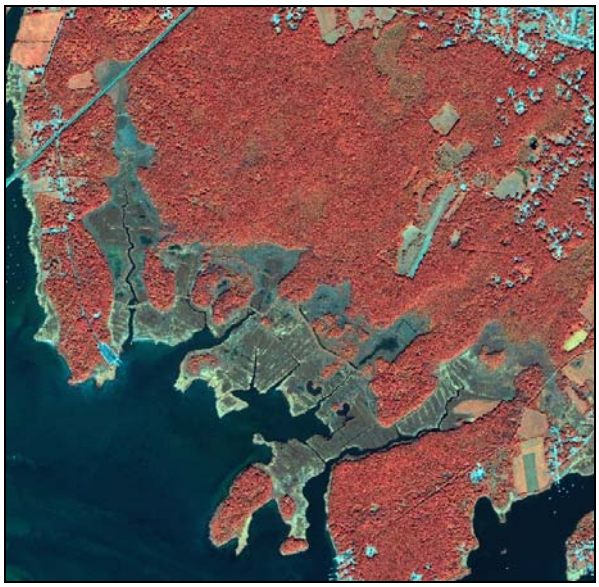

(b) QuickBird image the Barn Island Salt Marsh. Bands 4, 2, and 1. Acquired 28 September 2005.

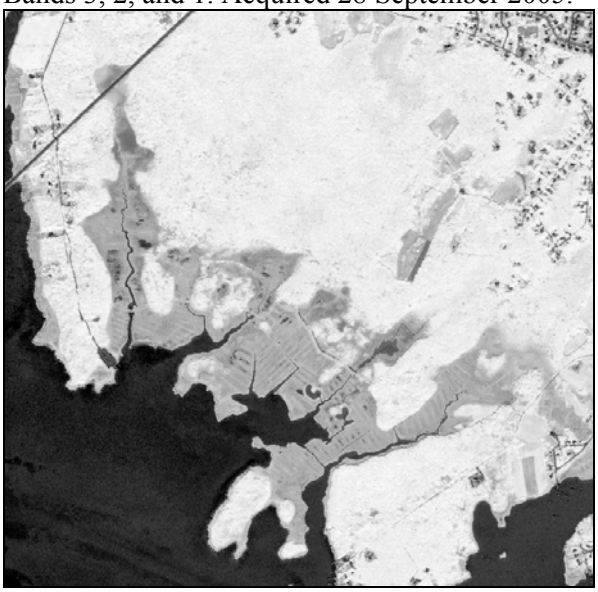

(c) Normalized Difference Vegetation Index (NDVI) of QuickBird image for the Barn Island Salt Marsh. Acquired 28 September 2005.

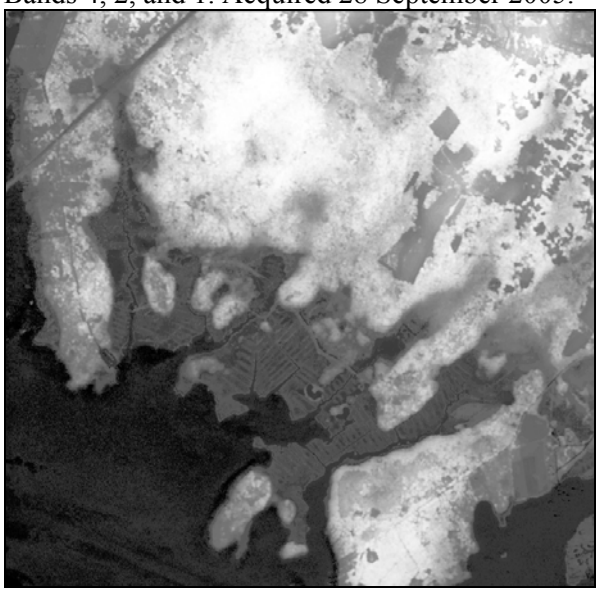

(d) Digital Surface Model (DSM) derived from ADS40 aerial image data for the Barn Island Salt Marsh. Acquired September 2004.

Figure 26. Examples of data used for the classification of tidal marshes for Barn Island Marsh, Stonington, CT.

See5 was used to assist in the derivation of rules (Figure 27) for classification with eCognition. For the coarser level segmentation, 1,011 examples of water, marsh, and other were used to train See5. Of the 14 attributes provided to See5, four were used in the separation of these classes: the Digital Surface Model, the near infrared reflectance (QuickBird band 4), the standard deviation of blue reflectance (band 2) within objects (an expression of texture), and NDVI, listed here in decreasing order of importance to the classification process.

The coarse level segmentation and classification resulted in an overall accuracy of 98.42% for the 1,011 training area objects (Table 15). For the marsh class, producer's accuracy, related to

errors of omission was 98.19%, and consumer's accuracy, related to errors of commission or false inclusions, was 95.18%. An assessment of the accuracy of the final image-wide classification using independent test data had not been conducted.

```
MeanADS40H > 3.78: Other (570)
MeanADS40H <= 3.78:
:...MeanNIR <= 127.52: Water (101/2)
    MeanNIR > 127.52:
    :...StdevBlue > 14.66: Other (73/2)
        StdevBlue <= 14.66:
        :...MeanNDVI > 199.39: Other (32/1)
            MeanNDVI <= 199.39:
            :...MeanADS40H <= 0.72: Marsh (195/6)
                MeanADS40H > 0.72:
                :...MeanNIR <= 259.11: Other (7)
                    MeanNIR > 259.11: Marsh (33/5)
```

Figure 27. Classification tree for QuickBird and DSM data for Barn Island: Coarse Objects and Three Classes.

Table 15. Accuracy assessment of coarse level segmentation of 28 September 2005 QuickBird imagery for Barn Island.

		Reference			
Classified As	**Water**	**Marsh**	**Other**	**Totals**	**Consumer's Accuracy**
Water	99	2	0	101	98.02%
Marsh	1	217	10	228	95.18%
Other	1	2	679	682	99.56%
Totals	101	221	689	1011	
Producer's Accuarcy	98.02%	98.19%	98.55%		

Overall Accuracy	98.42%

Figure 28 presents the coarse level classification results for the entire Barn Island Marsh as well as a detailed portion.

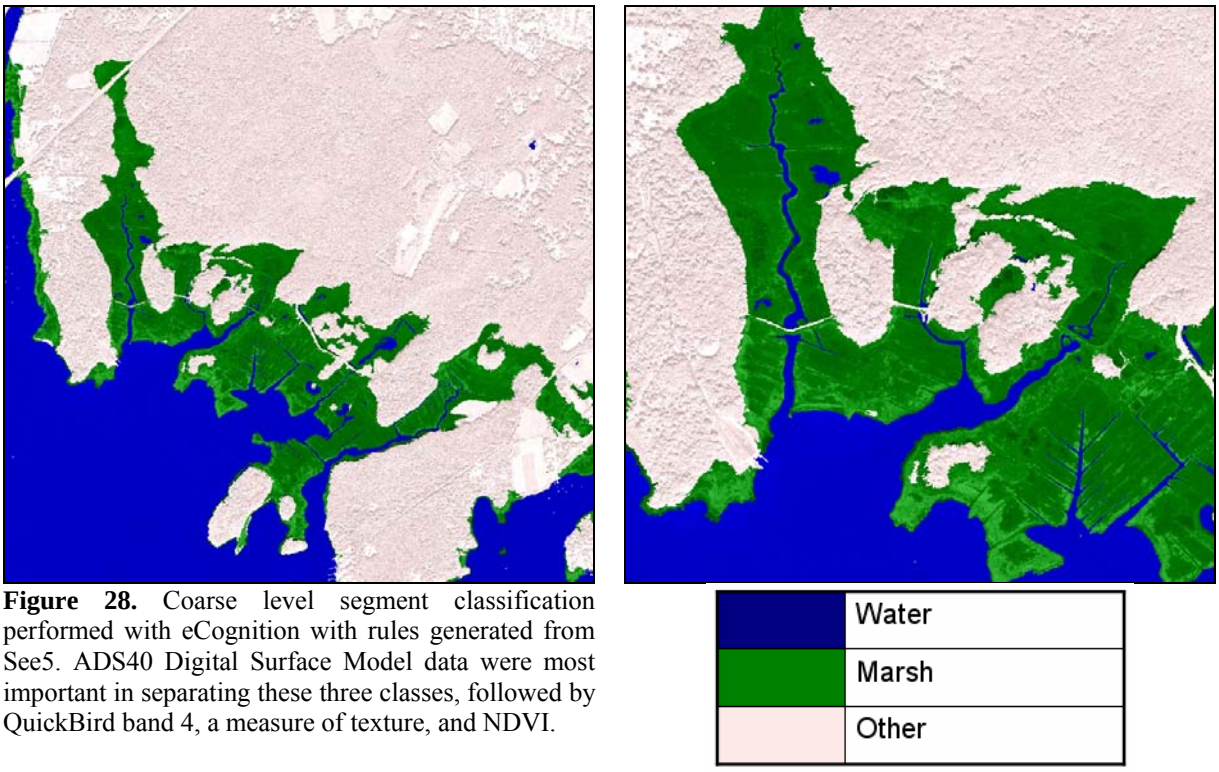

Figure 28. Coarse level segment classification performed with eCognition with rules generated from See5. ADS40 Digital Surface Model data were most important in separating these three classes, followed by QuickBird band 4, a measure of texture, and NDVI.

For the finer level of detail, which was both spatial and thematic, marsh, as classified in the coarser segmentation, was further divided into *Spartina alterniflora*, *Phragmites australis*, High Marsh Mosaic (consisting of *Spartina patens*, *Iva frutescens*, *Distichlis spicata*, *Juncus gerardi*), and mud(flats), and water was divided into ditch, creek, and open water.

Eight hundred objects were used to train See5 in developing the ruleset (Figure 29) for classifying these classes. Of 33 image attributes provided to See5, 12 were used in discriminating among the fine level classes, the top three being the standard deviation of red reflectance (band 3), the Digital Surface Model, and the green reflectance (band 2). Of the other nine variables, three were shape metrics and one was a texture measure.

The fine level segmentation and classification resulted in an overall accuracy of 91% for the 800 training area objects (Table 16). Producer's accuracy for *Phragmites australis* was 96.1% and consumer's was 94.8%, and for *Spartina alterniflora*, it was 88.5% and 96.7%, respectively. Figure 30 presents the fine level classification results for the entire Barn Island Marsh as well as a detailed portion.

Table 16. Error Matrix for Barn Island Classification.

Classified	Creek	High Marsh	Ditch	Mud	P. australis	S. alterniflora	Water	Totals	User's Accuracy
Creek	25					4		29	86.2%
High Marsh		127			2	33		162	78.4%
Ditch						14		14	0.0%
Mud				14		1		15	93.3%
P. australis		3			73	1		77	94.8%
S. alterniflora	4	9			1	406		420	96.7%
Water							83	83	100.0%
Totals	29	139	0	14	76	459	83	800	
Producer's Accuracy	86.2%	91.4%	n/a	100.0%	96.1%	88.5%	100.0%		

Overall Accuracy 91.0%

```
MeanNDVI <= 148.17:
:...MeanNIR <= 62.26: Water (83)
:   MeanNIR > 62.26:
:   :...MeanGreen > 194.23: Mud (14)
:       MeanGreen <= 194.23:
:       :...StdevGreen <= 5.9: Creek (29/4)
:           StdevGreen > 5.9: Spartina alterniflora (4)
MeanNDVI > 148.17:
:...MeanADS40H > 0.7:
    :...StdevGreen <= 11.33: Phragmites australis (71/2)
    :   StdevGreen > 11.33:
    :   :...GLCMEntrop <= 4.3: High Marsh Mosaic (13/2)
    :       GLCMEntrop > 4.3: Phragmites australis (5/1)
    MeanADS40H <= 0.7:
    :...MeanGreen <= 255.52: Spartina alterniflora (348/42)
        MeanGreen > 255.52:
        :...Length_wid > 3.23:
            :...MeanADS40H > 0.05: High Marsh Mosaic (5/2)
            :   MeanADS40H <= 0.05:
            :   :...MeanNDVI > 186.55: Spartina alterniflora (28/1)
            :       MeanNDVI <= 186.55:
            :       :...StdevGreen <= 17.59: High Marsh Mosaic (3)
            :           StdevGreen > 17.59: Spartina alterniflora (3)
            Length_wid <= 3.23:
            :...MeanNIR > 649.54: High Marsh Mosaic (21)
                MeanNIR <= 649.54:
                :...Borderleng <= 48:
                    :...MeanADS40H <= 0.01: Spartina alterniflora (30/3)
                    :   MeanADS40H > 0.01:
                    :   :...Borderleng <= 31.2: Spartina alterniflora (2)
                    :       Borderleng > 31.2: High Marsh Mosaic (3/1)
                    Borderleng > 48:
                    :...Rectangula <= 0.36: Spartina alterniflora (4)
                        Rectangula > 0.36:
                        :...MeanGreen <= 280.53:
                            :...MeanNIR > 475.24: Spartina alterniflora (9)
                            :   MeanNIR <= 475.24:
                            :   :...MeanNIR <= 405.02: High Marsh Mosaic (6)
                            :       MeanNIR > 405.02: [S1]
                            MeanGreen > 280.53:
                            :...MeanNDVI > 190.09: High Marsh Mosaic (21)
                                MeanNDVI <= 190.09:
                                :...MeanNDVI > 187.19: [S2]
                                    MeanNDVI <= 187.19: [S3]

SubTree [S1]

MeanNIR <= 436.56: Spartina alterniflora (14/4)
MeanNIR > 436.56:
:...StdevNDVI <= 1.88: Spartina alterniflora (4/1)
    StdevNDVI > 1.88: High Marsh Mosaic (17/2)

SubTree [S2]

MeanNIR <= 592.46: Spartina alterniflora (7/1)
MeanNIR > 592.46: High Marsh Mosaic (5/1)

SubTree [S3]

StdevGreen > 19.38: Spartina alterniflora (3/1)
StdevGreen <= 19.38:
:...GLCMEntrop <= 4.76: High Marsh Mosaic (32/1)
    GLCMEntrop > 4.76:
    :...Rectangula <= 0.72: High Marsh Mosaic (13/3)
        Rectangula > 0.72: Spartina alterniflora (3)
```

Figure 29. Classification tree for QuickBird and DSM data for Barn Island: Fine Objects and Seven Classes.

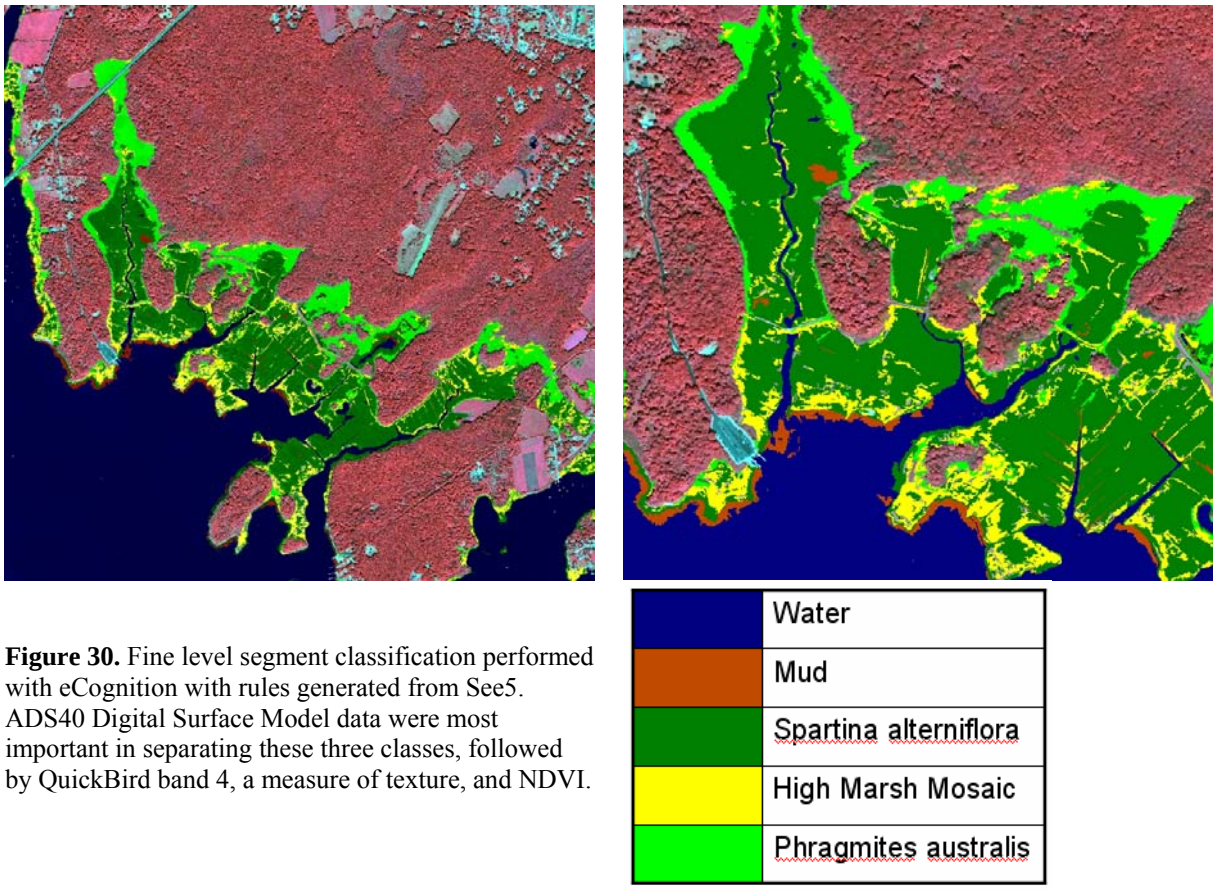

Figure 30. Fine level segment classification performed with eCognition with rules generated from See5. ADS40 Digital Surface Model data were most important in separating these three classes, followed by QuickBird band 4, a measure of texture, and NDVI.

Flax Pond: A single level hierarchical object-based classification was conducted for the Flax Pond marsh. eCognition software was used to perform an image segmentation using the four band John Deere Agri Services multispectral image, derived NDVI image, and derived principal components analysis band 1 image (PCA 1 produces a general overall brightness image). Segmentation parameters include a scale parameter of 60, color criteria of 0.9, shape criteria of 0.1 with a smoothness criteria of 0.9 and compactness criteria of 0.1. The input layers were all weighted to 1.0. Image objects that represented 11 land cover categories were selected as training data. For the classification process, the aforementioned data layers in addition to PCA 2, 3, and 4 and an elevation data digitized from a Digital Raster Graphic were included. The elevation information served to enhance the classification by providing additional separation among low elevation water and marsh categories from upland categories. A standard nearest neighbor classification was applied to the mean values of each data layer. Following the initial classification, the objects were further edited onscreen to eliminate classification errors. The resulting classification is provided in Figure 31. An overall accuracy is reported to be 87.50% based on 200 stratified random samples. The error matrix is provided in Table 17.

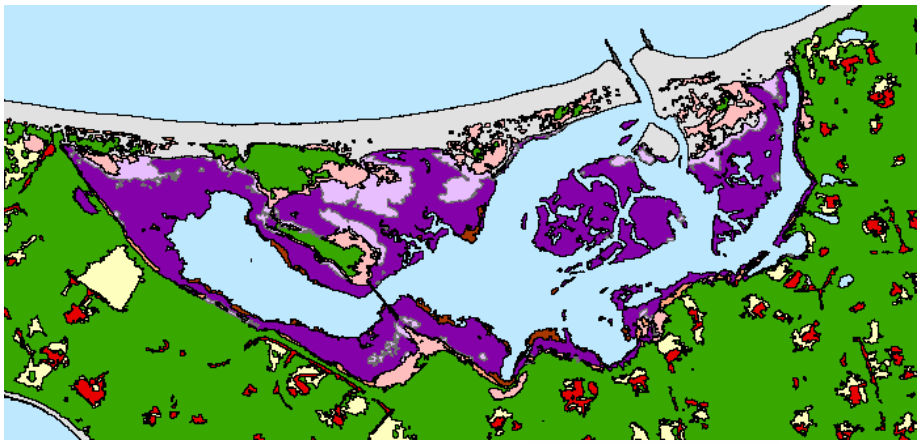

Object-based classification based on John Deere Agri Services digital imagery

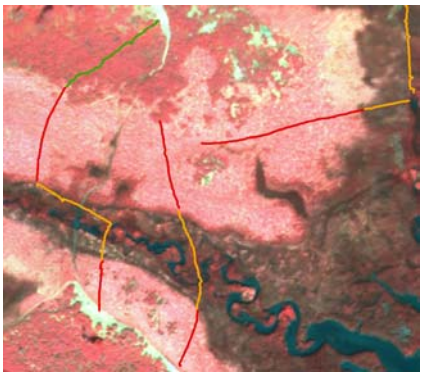

John Deere Agri Services digital image
September 18, 2006

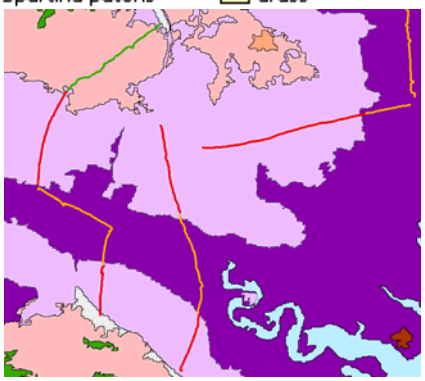

Object-based Classification

Colored vectors represent areas of different vegetation collected using a GPS receiver. Red identifies *S. patens,* orange identifies *S. alterniflora*, and green identifies *I. frutescens*

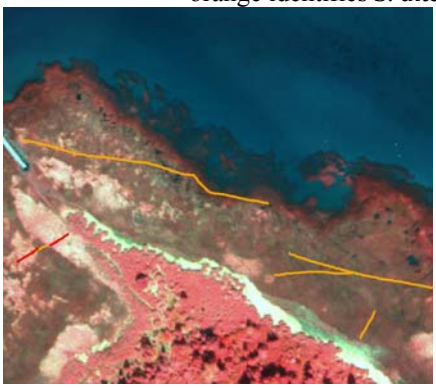

John Deere Agri Services digital image
September 18, 2006

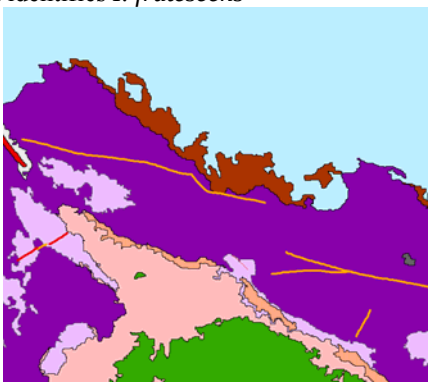

Object-based Classification

Colored vectors represent areas of different vegetation collected using a GPS receiver. Red identifies *S. patens,* and orange identifies *S. alterniflora*

Figure 31. Classification of John Deere imagery for Flax Pond, located on Long Island.

Table 10. Error matrix for John Deere classification of Flax Pond.

		Reference												
	CLASS	**1. Built-up**	**2. Forest**	**3. Water**	**4. Mud Flats**	**5. *S. alterniflora***	**6. *S. patens***	**7. *I. frutescens* /Scrb**	**8. Barren Sand**	**9. barren Rock**	**10. Wrack/Debris**	**11. Grass**	**TOTAL**	**User Accuracy**
Classified	**1**	13	0	0	0	0	0	0	0	0	0	0	**13**	**100**
	2	0	36	0	0	0	0	0	0	0	0	0	**36**	**100**
	3	0	0	36	0	0	0	0	0	0	0	0	**36**	**100**
	4	0	0	1	9	2	0	0	0	0	0	0	**12**	**75.0**
	5	0	1	0	1	10	0	0	0	0	0	0	**20**	**90.0**
	6	0	0	0	0	1	12	0	0	0	1	0	**14**	**85.7**
	7	0	1	0	0	1	1	8	3	0	0	0	**14**	**57.1**
	8	0	0	0	0	0	0	0	17	0	0	0	**17**	**100**
	9	0	3	0	0	0	0	0	0	7	2	0	**12**	**58.3**
	10	0	0	0	0	2	0	0	2	0	8	0	**12**	**66.7**
	11	0	3	0	0	0	0	0	0	0	0	11	**14**	**78.6**
	TOTAL	**13**	**44**	**37**	**10**	**24**	**13**	**8**	**22**	**7**	**11**	**11**	***200***	
	Producer Accuracy	**100**	**81.8**	**97.3**	**90.0**	**75.0**	**92.3**	**100**	**77.2**	**100**	**72.7**	**100**		

Number Correct = 175 out of 200
Overall Accuracy = 87.50%
Overall Kappa Statistic = 0.8583

Task 3. Determination of optimal spatial, spectral, and temporal resolutions for coastal wetland system characterization.

Coastal Marsh Classification

The primary considerations for selecting digital image data pertain to the spectral and spatial resolution of the data. The spectral resolution refers to the number of unique portions of the electromagnetic spectrum that are collected by a sensor. The spatial resolution refers to the size of the picture element or ground unit collected by the sensor. This project examined both moderate spatial resolution imagery (Landsat ETM and ASTER) for the purpose of identifying the location of coastal marshes within Long Island Sound, and high spatial resolution imagery (QuickBird, ADS40, John Deere AgriServices) for the purpose of mapping dominant marsh plant species for selected coastal marshes.

Findings from this project indicate that Landsat satellite imagery is moderately effective at identifying the presence of coastal marshes (larger then 2 acres) throughout the Sound, but is not effective at clearly delineating the full extent of the coastal marshes. Although spectrally capable, the spatial resolution (30 meters) was found to be a detriment when attempting to delineate accurately the extent of each individual coastal marsh. Problem areas were found to occur near the boundary between the tidal marshes and upland forested areas and within the high marsh complex where there is confusion between tidal marsh and upland features. Small tidal

marsh complexes are difficult to detect due to the spatial resolution of the Landsat sensor being larger then many of these marsh areas and the associated mixed pixels that subsequently occur. In addition, the distinction between high marsh and low marsh was not accurately determined. The problems with the spatial resolution were found to be compounded when using different Landsat scenes to attempt to monitor changes in the size and shape of the marshes. The Landsat derived data were, however, found to be effective at providing an assessment of marshes at potential risk of degradation due to surrounding anthropogenic activities and habitat.

ASTER satellite imagery, with its slightly better spatial resolution (15 meters) in three out of nine spectral bands was expected to provide improved classification results over the Landsat image classification. A side-by-side classification and comparison between the ASTER and Landsat ETM sensor found no significant improvement. Because of this, the Landsat ETM sensor would be a better choice for coastal marsh identification due to the fact that a single Landsat image would only be needed to cover almost the entire Long Island Sound compared to multiple ASTER images to cover the same area. In addition, more Landsat images are regularly collected for the Long Island Sound region.

It was not expected that the moderate spatial resolution imagery would be able to detect dominant marsh plant species in the coastal marshes of Long Island Sound due to the spatial resolution of these sensors on the relatively small size and vegetative complexity of the coastal marshes. To truly characterize the vegetation of the coastal marshes, higher spatial resolution imagery is needed. Although this research project was originally designed to examine only the QuickBird satellite sensor to assess its efficacy for classifying coastal marshes, due to acquisition problems and the availability of other sensor products, other sources of high spatial resolution imagery were also examined.

Findings indicate that higher spatial resolution digital imagery, whether it is from satellite (QuickBird 2.44 meter spatial resolution) or aircraft (ADS40 0.5 meter spatial resolution and John Deere AgriServices 0.3 meter spatial resolution) is capable of identifying the dominant plant species within the coastal marshes of Long Island Sound. Although having less spectral resolution than both the Landsat and ASTER images (four bands for the higher resolution images versus seven or nine bands for Landsat and ASTER, respectively), enough information was present to conduct a reasonable classification. While spectral data alone from these sensors could produce a highly accurate classification result, it was found that the addition of elevation data, in the form of LiDAR or the ADS40's Digital Surface Model (DSM) improved the classifications in terms of both helping to identify the low lying flat areas that constitute the marsh area and also with identifying variations in height of different marsh plant species.

Identification of Vegetation within Coastal Marshes

The spectral characteristics of vegetation are due to leaf pigments, plant structure (biomass and canopy architecture and cover) and plant health throughout the phenological cycle. The variability observed in individual reflectance spectra is replicated when these spectra are resampled to QuickBird (or other sensor) bands. Much of the spectral variability in the resampled data can be attributed to expected increases in plant pigments and biomass during the green-up phase of plant growth, and the decline of these parameters during senescence. The

magnitude and rate of these changes is found to differ in individual species allowing their spectral discrimination at specific times during the growing season.

Many studies have shown a correlation between the near-infrared reflectance of vegetation and biomass in general and in marsh species in particular (*e.g.* Drake, 1976; Hardisky *et al*., 1984; 1986; Gross *et al*., 1993; Zhang *et al*., 1997). This effect is seen in the resampled data where *P. australis* and *Typha spp.*, both dense monocultures ≥ 2 meters high, have higher NDVI, NIR/red and NIR/green values throughout the growing season than the low-growing *S. patens* (Figures 4a, 4b, 4e). NIR index values peak for *Typha spp.* in the mid- late-June, corresponding to field observations of peak plant heights of ≥ 2 meters, full development of flowers and wholly green leaves. *P. australis* displays peak NIR index values in mid-August to early-September correlating to peak plant heights of ≥ 3 meters and the development of flowers. Additionally, by late August, *Typha spp.* leaves are mostly brown, exacerbating the NIR distinction between the two species on this date. The differences in the timing of peak biomass between *Typha spp.* and *P. australis* were used to discriminate between these two species in the classification. The late season peak in NIR reflectance for *P. australis* (Artigas & Yang, 2005; 2006; Gao & Zhang, 2006) and its distinction from *Typha spp.* (Laba *et al*., 2005) has been noted in other marshes.

Some of the variability in the spectral indices can be correlated to genetic differences in pigment concentrations among the three species. The green/blue ratio of *S. patens* is dramatically higher than that of *P. australis* or *Typha spp.* from mid- June through late August (Figure 21c). We attribute this to inherent differences in the amount of chlorophyll *b* and carotenoids in these species, both of which absorb in the blue portion of the spectrum (Figure 20). This effect can be seen in the field, where both *P. australis* and *Typha spp*. leaves are observed to have a slight bluish hue. The peak in the green/blue index for *S. patens* in mid- July corresponds to maximum pigment concentration at this time of year. This is also the time of peak biomass of this species as recorded in the NIR ratios, however the NIR indices for *S. patens* are not distinct from the other species at this time.

Typha spp. also displays seasonal changes in pigment concentrations that were useful for classification. Values for the red/green index are higher for *Typha spp*. than the other species in early August (Figure 21d) likely due to a reduction in leaf chlorophyll pigments during senescence in this species at this time. The timing of *Typha spp.* senescence is also observed in the NIR and thus both the red/green and NIR/green indices were utilized to distinguish *Typha spp.* in the classification.

The resampled spectral data generate the following set of spectral rules that may be applicable to the distinction of *P. australis*, *Typha spp.* and *S. patens* communities: 1) *P. australis* is best distinguished by its high NIR response late in the growing season due to its high biomass especially with respect to the other species, 2) *Typha spp.* is best distinguished by NIR response in June and high red/green response in August which correspond to peak biomass and senescence, respectively, and 3) *S. patens* is best distinguished by pigment differences that result in a unique green/blue ratio throughout the growing season, peaking in July. These indices suggest that multispectral data such as QuickBird is adequate to measure and distinguish remotely the phenological spectral characteristics of these species. Silvestri (2002) shows that the error in field reflectance data is always greater than at larger scale, predicting that species

should be even more spectrally separable in image data than in the ground data. The data further suggest that if these phenological relationships hold from year to year, these rules can be applied to single date multispectral data to look for particular species. For example, our observations lead us to recommend acquisition of color infrared or four-band satellite data during late August to early-September to facilitate detection of *P. australis*.

The phenological trends seen here can vary as a function of plant vigor, which may depend on changes in salinity, weather, predation or disturbance. That these trends are consistent over two years at two separate areas of Ragged Rock Creek marsh suggests that these rules may have broader spatial and temporal application, but are perhaps best limited to regions of consistent climate.

The classification results indicate that *P. australis* is most accurately identified due to the fact that *P. australis* is generally a dense monoculture and that in the late summer it was observed to be approximately 1 m taller than the next tallest species. These characteristics combine to result in a high biomass and consequent NIR response that is greater than the other species. The plant height also distinguishes *P. australis* in the LiDAR data (Figure 32). While the use of LiDAR as a sole discriminant could identify a large proportion of *P. australis* occurrences, the spectral characteristics are necessary to distinguish between *P. australis* and *Typha spp.* because there is considerable overlap in the height data.

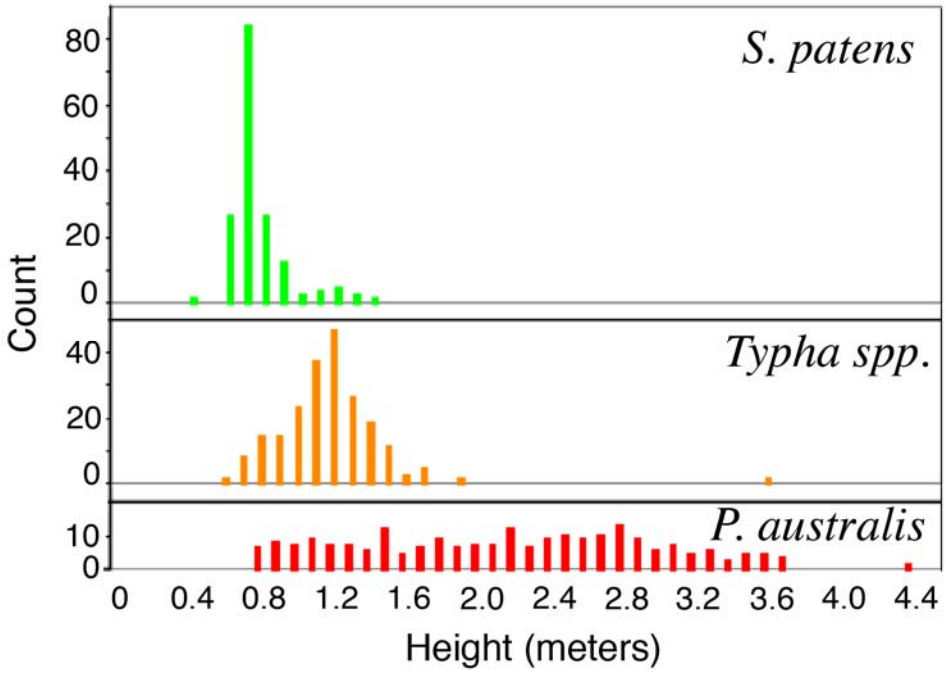

Figure 32. Histograms of the LiDAR height of each ground point displayed based on dominant class.

The validation results for all species improved when considering presence/absence of species in place of dominant species. Yu *et al.* (2006) report a criteria discrepancy when classifying vegetation using high-spatial resolution imagery and eCognition. They found that the criteria discrepancy between image classification and vegetation field mapping results in misleading

accuracies when traditional methods are employed. They found that when ecological associates are incorporated into accuracy assessment, the classification accuracy improved. Treating the validation points in this study as presence/absence had the same results. The greatest increase in accuracy was the reduction of commission errors for *S. patens*, which we suggest results from its distribution as understory in many of the validation quadrats. In these situations, the spectral signature of *S. patens* contributes to the signal even if taller species dominate the LiDAR first return (canopy) data. *S. patens* was most often confused for bare ground/flotsam/wrack, which are all low-lying and spectrally bright and for other low growing species such as blackgrass (*Juncus gerardii*), bentgrass (*Agrostis stolonifera*) and switchgrass (*Panicum virgatum*).

Typha spp. commission errors include *P. australis* and a number of other species. Many of these species, like *P. australis*, are observed to occur at similar heights (approximately 1 – 2 m) to *Typha spp*. during the middle part of the growing season, including sedges (*Schenoplectus* species) and bulrushes (*Bolboschoenus* species). The wide range of species that are confused with *Typha spp.* is likely exacerbated by the fact that it covers the most area of the marsh as well as its lack of an extreme, defining spectral or height rule. Both *P. australis* and *S. patens* have extremes in the LiDAR data (tallest and shortest, respectively) and have one band ratio that is quite distinct (late season NIR/red and mid-season green/blue, respectively). The lack of extreme spectral and height values for *Typha spp*. increases the potential for confusion and error.

The radiometry rules (Figure 21) make clear the necessity of multi-temporal imagery for mapping multiple species on a complex tidal marsh. When the objective is to map and isolate a single species such as *P. australis* for management, a single date of imagery could be adequate. However, the growth habit of the numerous marsh species on the Ragged Rock marsh necessitate multi-temporal data. Other studies have found similar benefit from incorporating multitemporal imagery into vegetation mapping (Carleer and Wolff, 2004; Dennison and Roberts, 2003).

Task 4. Outreach and Education Plan

The World Wide Web provides an excellent vehicle for the dissemination of information to a broad audience. As such, we have developed and published a website that provides the results and information regarding this project. The site can be accessed at:

http://clear.uconn.edu/projects/tidal_marsh/tidal_marsh.html

Within this site, information regarding the purpose of the project, data used for analysis and classification, results of classifications, comparison of various image types, and recommendations can be found. Figure 33 through 36 provide samples of the webpage content.

In addition to the dissemination via the website, information from this project will be incorporated into various ongoing educational programs within CLEAR. Most notably these include *Focus on the Coast*[8] and the *Community Resource Inventory*[9]. Further, the information derived in this project will be incorporated in NEMO Sea Grant educational programs focused on coastal communities.

[8] http://nemo.uconn.edu/tools/fotc/index.htm
[9] http://nemo.uconn.edu/tools/cri/index.htm

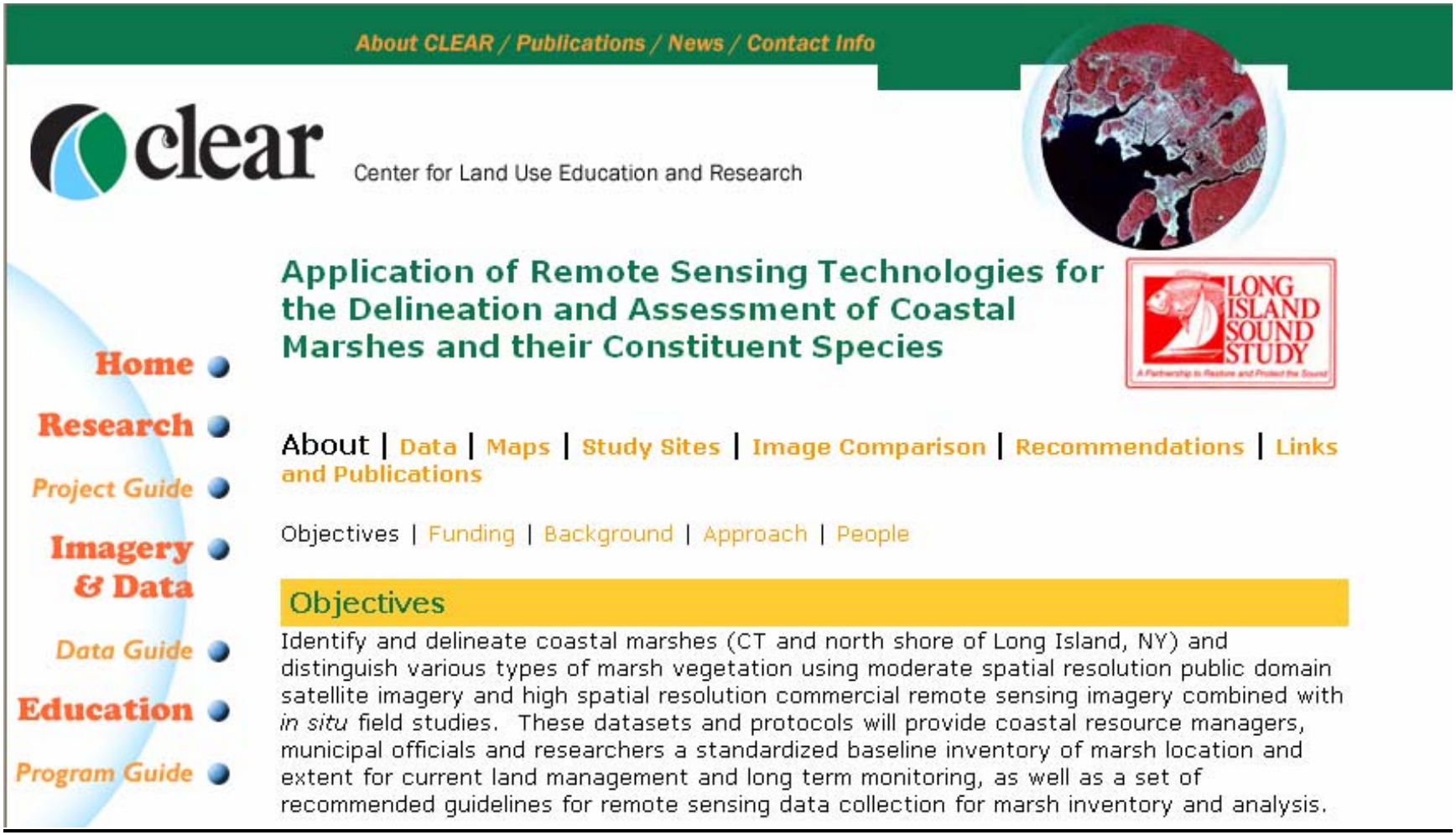

Figure 33. Project Homepage.

Imagery

Shown below are sample remote sensing images for selected salt marsh study sites. The spatial resolution of these data range from moderate (30 meters for Landsat) to high (0.3 meter for aerial imagery). All data are multispectral, consisting of three, four, or as many as six (reflective) bands. Also shown below are examples of the key salt marsh vegetation, shown on the remote sensing images, as well as field-based spectral reflectance and terrestrial potographs.

Remote Sensing Image Properties

Natural Color Imagery (Blue-Green-Red portion of the spectrum)
Click on a thumbnail for a full resolution image

Landsat QuickBird ADS40 John Deere

Color Infrared Imagery (Green-Red-Near Infrared portion of the spectrum)
Click on a thumbnail for a full resolution image

Landsat QuickBird ADS40 John Deere LIS Aerial

Figure 34. Project Website: Imagery comparison page.

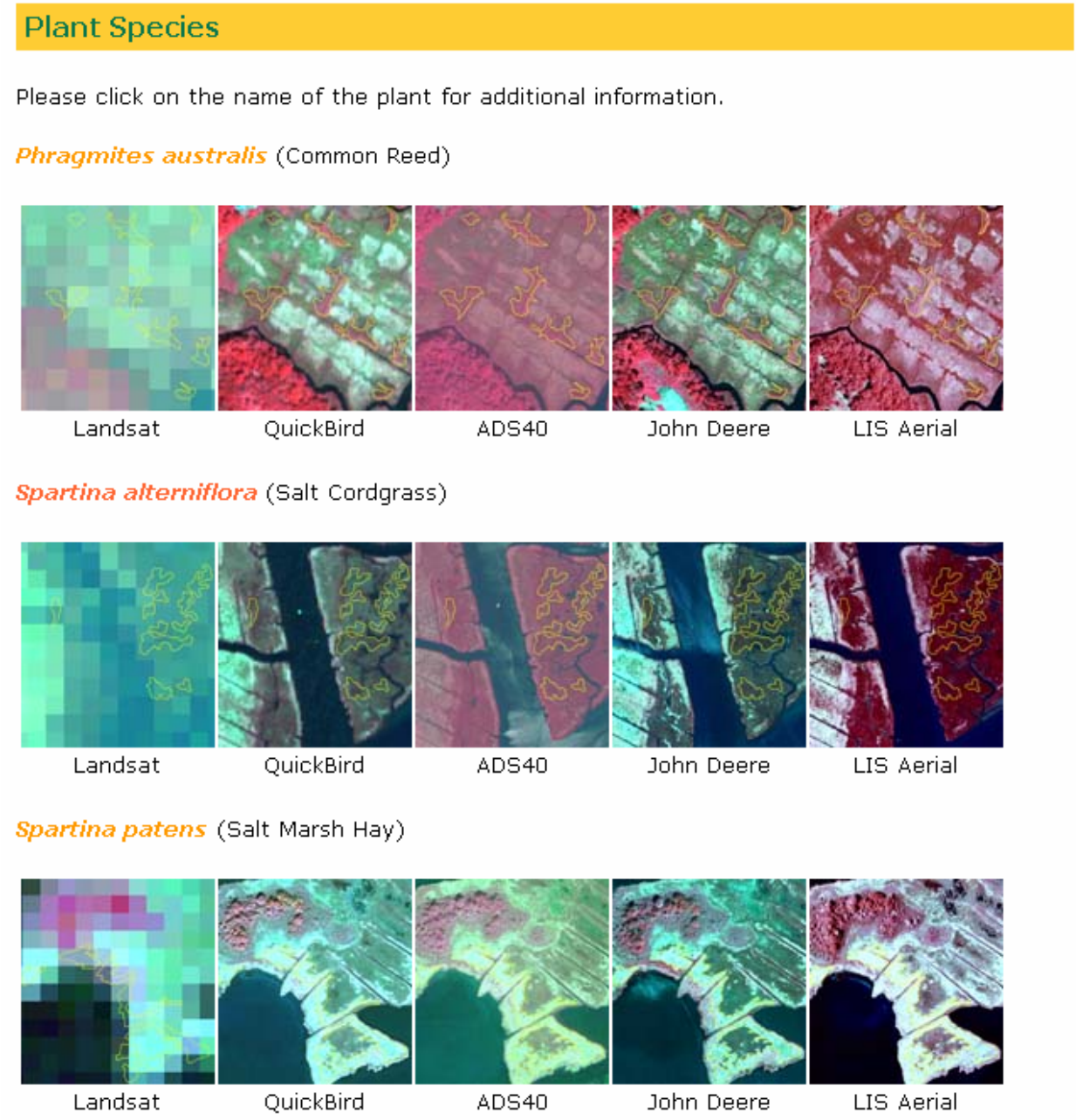

Figure 35. Project Website: Examples of salt marsh plant species in different remote sensing imagery.

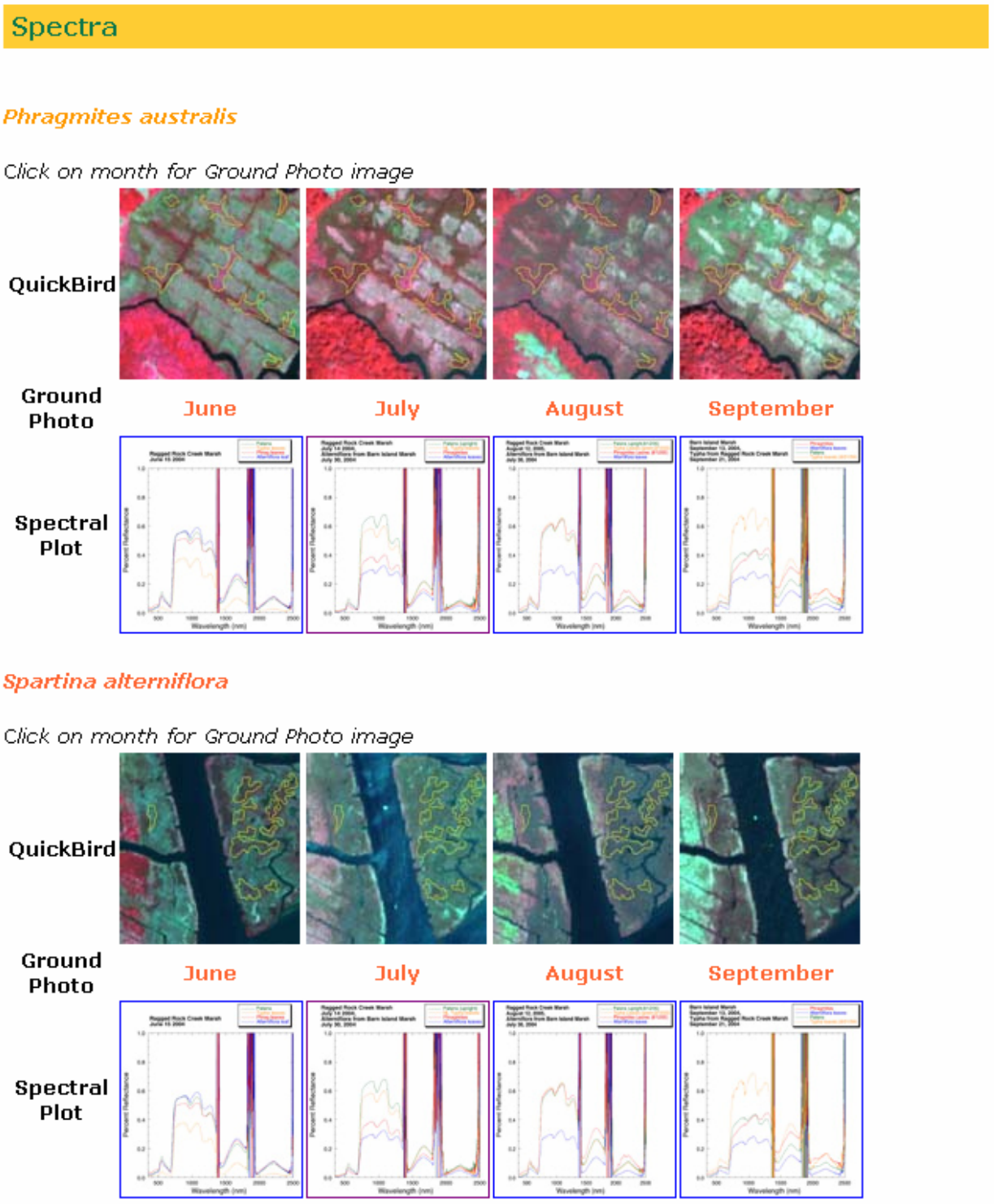

Figure 36. Project Website: Examples of salt marsh plant species in different times of the year and corresponding in situ spectral reflectance curves.

Summary of Findings and Recommendations

Delineation and monitoring of coastal marshes

We have developed semi-automated techniques for the classification of Landsat imagery into water, upland, and marsh categories. These techniques are based on pixel and object-oriented classification. The techniques have a high classification accuracy and are repeatable on images collected at different times. Using these techniques, we have produced a map that inventories the location of marshes around the whole of Long Island Sound in September of 2002 (Figure 8). These techniques could be applied to other Landsat images to track the distribution and extent of marshes over time although the spatial resolution of the Landsat image and the size of change occurring within the coastal marshes could become problematic (Figure 17).

A benefit of Landsat imagery is that a single path captures almost the entire Long Island Sound region (excluding the extreme eastern part of the Sound) thereby eliminating any temporal or radiometric resolution issues that are typical of aerial surveys. With a revisit time of every 16 days, acquisition of useable imagery is dependent on the atmospheric conditions of the area. If the timeframe is limited to just the July through September growing season, there is only the possibility of six or seven scenes that could be collected.

Landsat imagery, which has 30 meter spatial resolution, is useful for identifying the general location of coastal marshes but is too coarse to capture accurately their full extent and detail. ASTER imagery, while having higher spatial resolution in the visible to near-infrared portion of the electromagnetic spectrum did not perform any better in terms of classifying coastal marshes. A significant drawback to the ASTER imagery is the inconsistent temporal resolution (lack of quality growing season imagery) and the footprint size of the ASTER imagery (several scenes are required to cover the entire Sound area). QuickBird satellite imagery has a higher spatial resolution (2.44-meters multispectral) that is capable of capturing the full extent of the coastal marshes within the Long Island Sound area. Another advantage is the ability to point the sensor off nadir providing for additional opportunities for collection and avoiding poor atmospheric conditions. The drawbacks to the sensor are the north-south orientation of the path of the sensor thus requiring numerous scenes to be collected to cover the full extent of the Sound. It is extremely difficult to obtain a temporally consistent set of image data because of this.

The classification methodologies developed here for Landsat were combined with ancillary data sets such as elevation, impervious surface and other land cover classification to analyze a subset of marshes in the context of their surrounding land cover. Elevation data provide an advantage to the classification process as long as the data are of sufficiently small spatial resolution to have several data pixels fall within the upland boundaries of the coastal marsh. Additionally, the elevation accuracy is very important. This experiment was able to identify the relative magnitude of environmental pressures (*e.g.*, sea level rise, urban and suburban development) on each marsh (Figure 16). The combination of factors was used to derive an environmental risk assessment for select marshes. This could be used to 1) identify marshes that are in need of attention, 2) identify the possible causes for increased risk in each marsh, 3) monitor the changes in marsh health through time and in response to mitigation strategies. The analyses employed here are flexible, allowing the addition of other georeferenced data if such data were to become available (*e.g.*, pollutants).

The classification approaches used in this project can be adapted by other researchers in other GIS-based applications to address other environmental and management objectives.

Identification of vegetative species within marshes

We have developed a semi-automated classification methodology using QuickBird data to identify and differentiate the dominant species *P. australis*, *S. patens* and *Typha spp*. in Ragged Rock Creek Marsh. Critical to the success of this task was 1) the use of image data of high enough resolution to be comparable to the stands of plants under study (meter scale), and 2) documentation of the phenology of plants throughout the growing season to predict the spectral response of each species through time.

Our field surveys find that for Connecticut:

1. *P. australis* is best distinguished by its high NIR response late in the growing season due to its high biomass especially with respect to the other species.
2. *Typha spp.* is best distinguished by NIR response in June and high red/green response in August which corresponds to peak biomass and senescence, respectively.
3. *S. patens* is best distinguished by pigment differences that result in a unique green/blue ratio throughout the growing season, peaking in July.

The phenological variability seen in the field spectra was repeatable at Ragged Rock Creek over two field seasons, appears to be representative of the behavior of these species at other marshes in CT based on our more limited field surveys of 2004, and appears to coincide with the behavior of *P. australis* at NY and NJ marshes based on comparison to the literature (Artigas and Yang, 2005; 2006; Laba *et al*., 2005). To our knowledge, these are the only field spectra collected of marsh vegetation in CT, and as such should serve as a baseline for future remote sensing and ecological research. The spectra are inventoried and available on our web site for use by other researchers.

We have shown that the behavior the high spectral resolution field data is recognizable in the coarser spectral resolution QuickBird data and that high spatial resolution, moderate-resolution multispectral data such as QuickBird are adequate to measure and distinguish remotely marsh vegetation. This should also apply to other four-band data sets including NIR aerial photography, where, for example, *P. australis* could be recognized in the early fall as having the highest NIR response in a single image. The benefits of remotely sensed data over aerial photographs in this example are clear: 1) the remote sensing data are already radiometrically and geometrically corrected allowing mosaicking of scenes over larger areas than a single aerial photo, and 2) the remote sensing data allow for procedures such as ratioing that eliminate noise due to atmospheric variability.

The radiometry rules make clear the necessity of multi-temporal imagery for mapping multiple species on a complex tidal marsh due to the growth habit of the numerous marsh species. When the objective is to map and isolate a single species, a single date of imagery could be adequate. This is likely the case for the recognition of *P. australis*, where acquisition of a single date of imagery late in the growing season would be adequate for inventory and monitoring. For *P. australis* monitoring, we suggest that current aerial surveys be flown late in the growing season

and/or that these surveys be replaced by or augmented with high resolution satellite or aerial remote sensing data such as QuickBird, ADS40 or John Deere data. The advantages to the ADS40 and John Deere data over QuickBird are the higher spatial resolution and the temporal flexibility afforded by flying aerial surveys.

Top of canopy information derived from LiDAR or other data source capable of capturing plant canopies, such as ADS40 Digital Surface Model (DSM) data, is an added advantage for identifying various plant species. The success of using such information is dependent on the stem and crown density of the plant community being measured (areas with low plant density are not as easily identified) and there being sufficient height differences among the plants being classified.

Conclusions

Remote sensing is a powerful tool for the classification of land cover. It offers a synoptic view of a large region, the data are acquired through time and the data are in a format that is compatible with a variety of georeferenced data sets. In this project, we sought to determine how best to utilize these data to inventory marshes around the whole of Long Island Sound. Such an inventory is a fundamental data set for research scientists and managers necessary to map the distribution of marshes through time. We have found that 30 m Landsat data is adequate to distinguish marshes from upland areas and water. The data have the benefit of being low cost (~$400/scene) and cover large contiguous regions of the Sound. The classification methodology developed here has high accuracy and is found to be repeatable on images acquired on different dates.

We combined the Landsat classification with other data sets to evaluate several environmental and anthropogenic factors affecting a subset of marshes. This is possible because of the spectral and spatial information contained in remote sensing data, allowing the identification of variables (*e.g.*, land cover) and their effect on marsh health (*e.g.*, proximity). The data sets were combined to produce a marsh risk assessment, which could be very useful to land managers seeking to understand marsh health and evaluate remediation efforts. The data sets themselves also provide information to scientists as to the types and influence of various factors on marsh health. Thus, both the classified Landsat image provided in Figure 8a and the methodology utilizing multiple remote sensing and spatial data sets directly addresses fundamental questions about the marshes: where are they, how healthy are they, and are they changing? Detailed field surveys, which are not routinely conducted for all of the marshes throughout the year, will add valuable information to place these larger data sets in context and *vice versa*.

We find that high resolution (meter scale) remote sensing data are adequate to inventory major vegetative species within individual marshes. These image data are classified based on our new understanding of the variation in the spectral reflectance properties of each species throughout the growing season determined by *in situ* radiometric measurements in the field. These field spectra are unique in Connecticut and can serve as a baseline for research on the phenological variability of major marsh species. We have demonstrated that the spectral variability seen in the field is also apparent at the sensor. The field data show that *S. patens*, *Typha spp*. and *P. australis* are spectrally recognizable and distinct from one another at certain times of year. *P.*

australis is best recognized by its high NIR response late in the growing season. Thus it should be recognizable in a variety of data sets that include NIR reflectance. As the invasive *P. australis* is of concern to managers and is actively being remediated across Connecticut, the classification methods outlined here offer a new way to inventory *P. australis* and monitor its change through time.

These image data and classification technologies developed here provide the tools to assess routinely the distribution of coastal marshes and *P. australis* within those marshes. These data are critical to understanding the forces driving environmental change and to evaluate and guide management practices. We recommend acquisition of the following data sets to continue to make these measurements through time:

1. Annual acquisition and classification of Landsat images for marsh inventory. 3 Landsat scenes are required to cover the whole of Long Island Sound @ ~ $400 per scene. The scenes should be acquired sometime during the growing season when the marshes contain live vegetation.
2. Replacing or augmenting current aerial photo surveys with high resolution (submeter) aerial multispectral digital images of entire coast to inventory *P. australis* and other species. To identify *P. australis*, the survey should be in late August/ early Sept. The cost of ADS40 image data for 36 coastal communities = $100K.

Presentations/Publications/Outreach

Gilmore, M.S., E.H. Wilson, D.L. Civco, S. Prisloe, N. Barrett, J.D. Hurd, and C. Chadwick. (2007). Integrating multi-temporal spectral and structural information to map dominant tidal wetland vegetation in a lower Connecticut river marsh, submitted to *Remote Sensing of Environment*, special issue: "Applications on Remote Sensing to Monitoring Freshwater and Estuarine Systems." (in press)

Gilmore, M.S., D.L. Civco, E.H. Wilson, J.D. Hurd, S. Prisloe, C. Chadwick, and N. Barrett (2007). Object-oriented classification and mapping of salt marsh vegetation using in situ radiometry and multiseasonal, high resolution satellite remote sensing data. Proc. *MultiTemp 2007: The Fourth International Workshop on the Analysis of Multi-temporal Remote Sensing Images*. Leuven, Belgium, 7 pp.

Civco, D.L., J.D. Hurd, S. Prisloe, and M.S. Gilmore (2006). Characterization of coastal wetland systems using multiple remote sensing data types and analytical techniques. *Proc. IEEE International Geoscience and Remote Sensing Symposium*, Denver, CO, 5 pp.

Hurd J.D., D.L. Civco, M.S. Gilmore, S. Prisloe and E.H. Wilson (2006). Tidal wetland classification from Landsat imagery using and integrated pixel-based and object-based classification approach. *Proc. 2006 ASPRS Annual Conference*, Reno, NV, 11 pp.

Prisloe, S., E.H. Wilson, D.L. Civco, J.D. Hurd and M.S. Gilmore (2006). Use of LIDAR data to aid in discriminating and mapping plant communities in tidal marshes of the lower Connecticut river: Preliminary results. *Proc. 2006 ASPRS Annual Conference*, Reno, NV, 8 pp.

Hurd J.D., D.L. Civco, M.S. Gilmore, S. Prisloe, and E.H. Wilson (2005). Coastal Marsh Characterization Using Satellite Remote Sensing and *In Situ* Radiometry Data: Preliminary Results. *Proc. 2005 ASPRS Annual Convention*, Baltimore, MD, 12 pp.

References

Artigas, F.J. and J.S. Yang (2005). Hyperspectral remote sensing of marsh species and plant vigour gradient in the New Jersey Meadowlands. *International Journal of Remote Sensing 26*, 5209-5220.

Artigas, F.J. and J.S. Yang (2006). Spectral discrimination of marsh vegetation types in the New Jersey Meadowlands, USA. *Wetlands 26*, 271-277.

Barrett, N. and S. Prisloe (1998). Spatial patterns of expansion of by *Phragmites australis* (Cav.) Trin. Ex Steud. within the tidelands of the Connecticut River from 1968 to 1994. CD-ROM and report to The Nature Conservancy, Middletown, CT, 1 June 1998.

Benz, U.C., P. Hofmann, G. Willhauck, I. Lingenfelder, and M. Heynen (2004). Multi-resolution, object-oriented fuzzy analysis of remote sensing data for GIS-ready information. *Photogrammetry and Remote Sensing 58*, 239-258.

Bertness, M.D., P.J. Ewanchuk and B.R. Silliman (2002). Anthropogenic modification of New England salt marsh landscapes. *PNAS 99,* 1394-1398.

Carleer, A. and E. Wolff (2004). Exploitation of very high resolution satellite data for tree species identification. *Photogrammetry and Remote Sensing 70*, 135-140.

Chambers, R.M., L.A. Myerson and K. Saltonstall (1999). Expansion of *Phragmites australis* into tidal wetlands of North America. *Aquatic Botany 64,* 261-273.

Congalton, R.G. and K. Green (1999). Assessing the Accuracy of Remotely Sensed Data: Principles and Practices. Lewis Publishers, Boca Raton, FL, 160 pp.

Dennison, P.E. and D.A. Roberts (2003). The effects of vegetation phenology on endmember selection and species mapping in southern California chaparral. *Remote Sensing of Environment 87,* 295-309.

Donnelly, J.P. and M.D. Bertness (2001). Rapid shoreward encroachment of salt marsh cordgrass in response to accelerated sea-level rise. *PNA 98,* 14218-14223.

Drake, B.G. (1976). Seasonal changes in reflectance and standing crop biomass in three salt marsh communities. *Plant Physiology 58*, 696-699.

Farnsworth, E.J. and L.A. Meyerson (1999). Species composition and inter-annual dynamics of a freshwater tidal plant community following removal of the invasive grass, *Phragmites australis*. *Biol. Invasion 1,* 115-127.

Gao, Z.G. and L.Q. Zhang (2006). Multi-seasonal spectral characteristics analysis of coastal salt marsh vegetation in Shanghai, China. *Estuarine, Coastal and Shelf Science 69*, 217-224.

Gross, M.F., M.A. Hardisky, P.L. Wolf, and V. Klemas (1993). Relationship among *Typha* biomass, pore water methane, and reflectance in a Delaware (U.S.A.) brackish marsh. *Journal of Coastal Research 9,* 339-355.

Hardisky, M.A., F.C. Daiber, C.T. Roman, and V. Klemas (1984). Remote sensing of biomass and annual net primary productivity of a salt marsh. *Remote Sensing of Environment 16,* 91-106.

Hardisky, M.A., M.F. Gross, and V. Klemas (1986). Remote sensing of coastal wetlands. *Bioscience 36*, 453-460.

IPCC. 2007. Climate Change 2007. The Physical Basis-Summary for Policymakers Accessed at http://www.ipcc.ch/SPM2feb07.pdf

Laba, M., F. Tsai, D. Ogurcak, S. Smith, and M.E. Richmond (2005). Field determination of optimal dates for the discrimination of invasive wetland plant species using derivative spectral analysis. *Photogrammetric Engineering and Remote Sensing 71*, 603-611.

Mimuro, M. and T. Katoh (1991). Carotenoids in photosynthesis: absorption, transfer and dissipation of light energy. *Pure and Applied Chemistry 63*, 123-130.

Moore, H.H., W.A. Niering, L.J. Marsicano, and M. Dowdell (1999). Vegetation change in created emergent wetlands (1988-1996) in Connecticut (USA). *Wetlands Ecol. Manag. 7,* 177-191.

Niering, W.A. and R.S. Warren (1980). Vegetation patterns and process in New England salt marshes. *BioScience* 30, 301-307.

Orson, R.A. (1999). A paleoecological assessment of *Phragmites australis* in New England tidal marshes: Changes in plant community structure during the last few millennia. *Biol. Invasions 1,* 149-158.

Roman, C.T., W.A. Niering, and R.S. Warren (1984). Salt marsh vegetation change in response to tidal restriction. *Environmental Management* 8, 141-150.

Silvestri, S., M. Marani, J. Settle, F. Benvenuto, and A. Marani (2002). Salt marsh vegetation radiometry Data analysis and scaling. *Remote Sensing of Environment 80*, 473-482.

Singh, A. (1989). Review Article Digital change detection techniques using remotely-sensed data. *International Journal of Remote Sensing* 106, 989 – 1003.

Warren, R.S. (1994). *Phragmites australis* on the tidelands of the lower Connecticut River: patterns of invasion and spread. Report to the Nature Conservancy Connecticut Chapter Conservation Biology Research Program. Middletown, CT; 20 pp.

Wooley, J.T. (1971). Reflectance and transmittance of light by leaves. *Plant Physiology 47*, 656-662.

Yu, Q., P. Gong, N. Clinton, G. Biging, M. Kelly, and D. Schirokauer (2006). Object-based detailed vegetation classification with airborne high spatial resolution remote sensing imagery. *Photogrammetric Engineering and Remote Sensing 72*, 799-811.

Zhang, M., S.L. Ustin, E. Rejmankova, and E.W. Sanderson (1997). Monitoring Pacific coast salt marshes using remote sensing. *Ecological Applications 7*, 1039-1053.